



Review

## Formation and application of porous silicon

H. Föll\*, M. Christophersen, J. Carstensen, G. Hasse

Faculty of Engineering, University of Kiel, Kaiserstrasse 2, D-24143 Kiel, Germany

### Abstract

All manifestations of pores in silicon are reviewed and discussed with respect to possible applications. Particular emphasis is put on macropores, which are classified in detail and reviewed in the context of pore formation models. Applications of macro-, meso-, and micropores are discussed separately together with some consideration of specific experimental topics. A brief discussion of a stochastic model of Si electrochemistry that was found useful in guiding experimental design for specific pore formation concludes the paper.

© 2002 Published by Elsevier Science B.V.

*Keywords:* Electrochemistry; Microstructure; Self-organization; Porous silicon

## 1. Introduction

### 1.1. Scope and aim of the paper

The electrochemistry of Si (and of other semiconductors) exhibits a large range of peculiar phenomena, many of which are not well understood at present. The most prominent feature under anodic etching conditions is the formation of pores and “porous silicon” has attracted increasing interest for a wide spectrum of potential applications since the discovery of the unexpected optical properties of microporous Si in 1990 [1,2]. In this paper, we endeavor to cover applications of porous Si, and since there are several recent papers dealing with properties and applications of microporous Si [3–8], the focus of this paper will be on everything else, i.e. on mesoporous and macroporous Si.

The parameter space for pore formation is very large and has not been fully explored. As shown in recent papers [9–12], it is still possible to find new kinds of pores in Si with peculiar features that may be of interest for applications. We will therefore review and classify the many types of pores that have been observed.

The Si–electrolyte contact, however, has more to offer to science and technology than just pore formation. Specific features with potential uses include:

- ohmic or diode-type contacts with obvious potential for applications [13],
- interfaces with an extremely low density of interface states and therefore very low values of the surface recombination velocity [14–16],
- solar cell like behavior, i.e. photo currents which may increase linearly or non-linearly with the light intensity [17],

\* Corresponding author. Tel.: +49-431-880-6175.

E-mail address: hf@tf.uni-kiel.de (H. Föll).

- anodic oxide formation in various modes [18],
- strong non-linear response to frequencies superimposed on voltages or currents as a relatively new issue [12–20],
- very peculiar anisotropies of certain properties, in particular macropore growth [21,22],
- self-induced current or voltage oscillations in certain areas of the parameter space for constant external voltage or current, respectively (referred to as potentiostatic or galvanostatic conditions), cf. [23,24].

All points, except the last two, have found applications (at least in proposals), and it is quite possible that new features will be added to this list in due time. So far, e.g. no self-ordered pore arrays have been observed as reported for  $\text{Al}_2\text{O}_3$  [25] or, more to the point, for GaAs [26,27], GaP [28,29] or InP [30,31]—always occurring with self-induced voltage oscillations (cf. Fig. 29). Will we be able to find self-ordered pores in Si, too? Also in connection with voltage oscillations? If not—why not? Nobody knows—and nobody is able to make a convincing prediction. This example serves to highlight our present level of the understanding of pore formation and to emphasize the viewpoint of the authors: pore formation in Si and all the other phenomena listed above (especially oscillations) are closely related.

This is a departure from more conventional approaches that try to model pore formation independently of all the other phenomena. We will therefore include the present status of a general model of the electrochemistry of Si in a final section and apply it to pore formation in Si.

Making porous Si in one of its many manifestations demands specific sets of parameters and some control of the etching process. While some pore morphologies are unique expressions of special parameters, others can be obtained for many, sometimes widely different conditions. With applications in mind, which set of parameters is best suited to the task—including economic considerations? While there are no simple answers at present, some guidelines can be given. The second section therefore attempts to correlate the zoology of macropores in Si and the most important ingredients from the available parameter space.

The third section deals with applications of macropores, the fourth and fifth with mesopores and micropores, respectively. While we try to review all potential applications presently pursued in the scientific/engineering communities together with specific problems, open questions, and emerging applications, it goes without saying that there are certainly some activities in the laboratories that the authors are not aware of—either because we failed to notice them or because they are (totally or partially) kept confidential on purpose. To compensate for this, there are some unpublished results that the authors are aware of and that will be included. In total, we cannot claim completeness in the listing of the application oriented work in this field and not always substantiate certain statements by citations.

### 1.2. Pores, electrolytes, and nomenclature

There is a large and growing diversity of pores in Si. Typical dimensions from 1 nm to 10  $\mu\text{m}$  and morphologies from sponge-like to perfect-cylindrical are encountered. In what follows we will first define some terms useful for discussing the geometry and morphology as well as the production and application of pores. First, we will distinguish the three major types of electrolytes in use today.

- Electrolytes derived from the  $\text{HF-H}_2\text{O}$  system; called “aqueous electrolytes” and abbreviated with “aqu”. This includes not only all mixtures of HF (commonly 49% p.w.) with water, but also fluorine bearing salts dissolved in  $\text{H}_2\text{O}$  (e.g.  $\text{NH}_4\text{F}$ ), additions of ethanol ( $\text{C}_2\text{H}_5\text{OH}$ ) and/or acetic

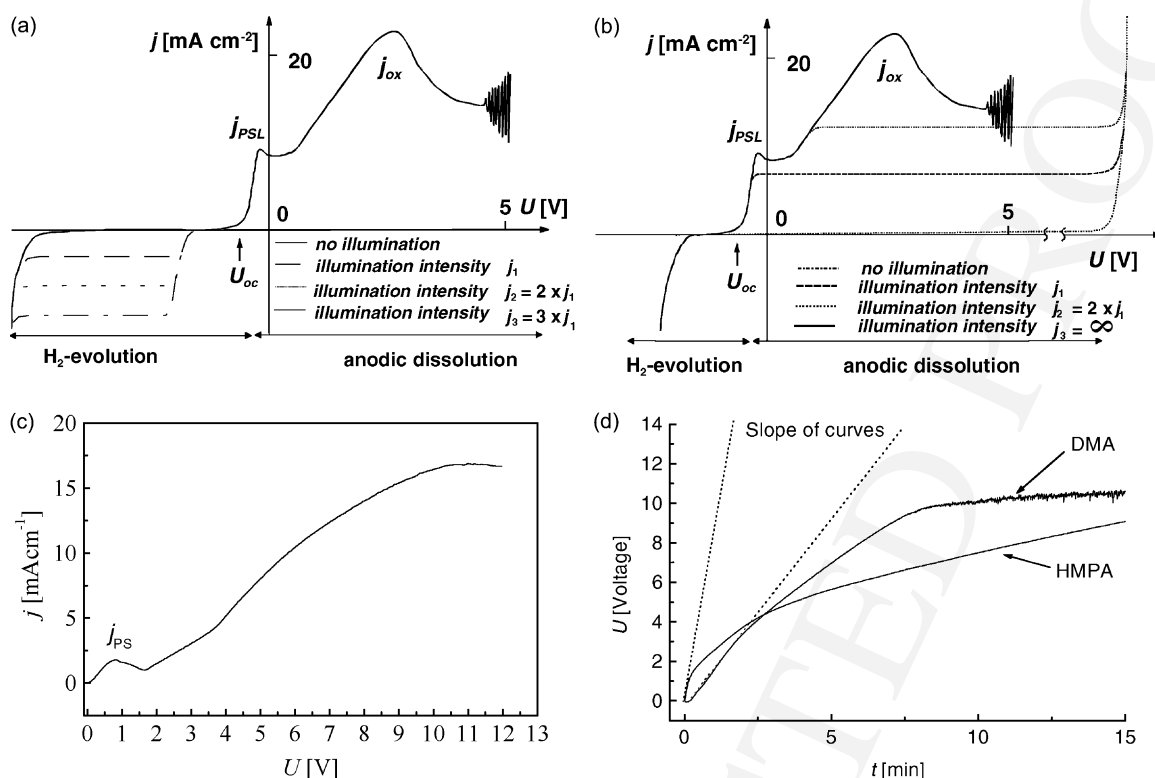


Fig. 1. Representative  $I(V)$  characteristics: (a) aqu electrolyte, p-type Si; (b) aqu electrolyte, n-type Si; (c) org electrolyte (FA); (d)  $U(t)$  for ox electrolytes. The PSL-peak is indicated by  $j_{PSL}$ .

80 acid (C<sub>2</sub>H<sub>4</sub>OH), or anything else that serves to reduce surface tension, adjusts the pH-value or the  
 81 viscosity, or simply helps to get the desired results for unknown reasons. The nominal  
 82 concentration of F (in any form) may range from 0.001 to 49%. All aqueous electrolytes have in  
 83 common that a “PSL-peak” (see Fig. 1) is found in the  $I(V)$ -characteristics and that they are rather  
 84 strongly oxidizing, i.e. tend to form SiO<sub>2</sub>.

• Electrolytes mixing HF and an organic solvent (always including some water coming from adding  
 86 HF (49%)). This class will be called “organic electrolytes” (“org” for short). There is a large  
 87 number of organic solvents that have been used; most prominent, perhaps, is acetonitrile (MeCN),  
 88 dimethylformamide (DMF), and dimethylsulfoxide (DMSO). While there might be some  
 89 confusion with HF/ethanol mixtures which we count among the aqu electrolytes as explained  
 90 above, the meaning is sufficiently clear in practice. Organic electrolytes so far have in common  
 91 that their  $I(V)$ -characteristics do not show a PSL-peak. While it is possible that the PSL-peak is  
 92 actually there but hidden due to the usually large resistance of the org electrolytes (which means  
 93 that the series resistance of the system dominates the characteristics), it will be reasoned in  
 94 Section 2 that this is a decisive feature of most (not necessarily all) org electrolytes and intimately  
 95 linked to their “oxidizing power” (see later), which can be rather small. In any case, the absence  
 96 of a PSL-peak gives a clear signal that formation models intimately tied to the current density  $j_{PSL}$   
 97 at the PSL-peak are limited in their application range.

• Electrolytes for anodic oxidation (called *oxidizing electrolytes*; abbreviated “ox”); always without  
 99 F<sup>-</sup> ions and containing some oxidizing reagent. Most common electrolytes without a HF addition  
 100 fall into this category and we may classify their “oxidizing power” according to how well they

101 form an oxide on Si. In practical terms, this is easily measured by performing a constant current  
102 experiment. Due to the oxide being formed (but not dissolved), the voltage has to rise in order to  
103 keep the current constant. In the beginning of such an experiment, the  $V(t)$ -curves are always  
104 linear and the value of the slope  $dV/dt$  will be used as a measure of the “oxidizing power” of the  
105 oxidizing electrolytes, Fig. 1d shows some typical characteristics. “Oxidizing power” in the  
106 context of this paper is thus a well defined entity and will now be used without quotation marks in  
107 the remainder of the paper. Pure ox electrolytes have only limited applications, but may provide a  
108 key for the understanding of the electrochemistry of Si.

109 There is one more (potentially large group) of electrolytes not covered in this scheme which one  
110 might call “mixed electrolytes”. This set contains everything not contained in the sets defined  
111 above, but so far not much practical significance has emerged. Examples that can be found in the  
112 literature include  $H_3PO_4$  (by itself an “ox” electrolyte) with a dash of HF [32], absolutely water  
113 free org electrolytes [33], or diluted HF with some  $CrO_4$  [34]. As the need arises, we will pinpoint  
114 these cases by mixing the symbols; the latter electrolyte than is designated (aqu + ox).

115 Next, we define some nomenclature regarding pores. According to the IUPAC standard, we  
116 must distinguish three categories by looking only at the parameters (average) pore diameter and  
117 (average) distance between pores, i.e. at the *geometry* of the pores.

- *Micropores*, with pore diameters and pore distances (from now on subsumed under “geometries”)  
119 <10 nm.
- *Mesopores*, with geometries in the 10–50 nm region.
- *Macropores* with geometries in the >50 nm region.

122

123 Note that the *geometry* of pores does not contain much information about their *morphology*.  
124 This term will be used as the collective identifier for properties like the shape (smooth, branched,  
125 faceted, . . .), orientation, or interaction of pores, that are independent of the geometry.

126 All three kinds of pores can be obtained under a variety of (sometimes very different)  
127 conditions, and with widely differing morphologies. Key parameters are the electrolyte type (aqu,  
128 org, ox), the HF concentration, the doping type and level of the Si ( $n$ ,  $n^+$ ,  $p$ ,  $p^+$ ), and in some cases  
129 the illumination state (back side illumination (bsi), or front side illumination (fsi)). We will use these  
130 abbreviations to extend the classification of pores in a self-explaining notation:  $n$ -macropores(aqu/  
131 bsi) or  $n$ -macropores(aqu/fsi) thus are macropores produced in  $n$ -Si under backside or frontside  
132 illumination using aqueous electrolyte;  $p$ -macropores(aqu) or  $p$ -macropores(org) denote macropores  
133 obtained without illumination in  $p$ -type Si with aqueous or organic electrolytes; and  $n^+$ -  
134 macropores(aqu + ox) denotes macropores obtained in heavily doped  $n$ -type Si in a mixture of an  
135 aqueous electrolyte with the addition of an oxidizing electrolyte, respectively.

136 It is absolutely essential to adhere to this nomenclature to avoid considerable confusion—the  
137 examples chosen demonstrate this point: macropores can be obtained under a variety of very  
138 different conditions; Fig. 2 illustrates this. This was a rather unforeseen development since the  
139 discovery of smooth cylindrical (“perfect”)  $n$ -macropores(aqu/bsi) with large aspect ratios by  
140 Lehmann and Föll in 1990 [35]. While this kind of macropores was investigated in some detail, only  
141 few investigations dealt with the rest.

142 The basic IUPAC distinction of pores into micro-, meso-, and macropores is far to coarse and  
143 not particularly well suited to unambiguously sort out pores in Si. The term “macropore” usually is  
144 associated with smooth cylindrical pores in the 1  $\mu$ m region, and no such macropores have been  
145 observed (so far) in the 50 to 500 nm region to which the term nominally applies. Contrariwise,  
146 while  $n^+$ -,  $p^+$ -mesopores(aqu) are indeed (mostly) found within their admissible size range of 10–  
147 50 nm, it is simply not useful to call pores “macropores” that have a morphology exactly like

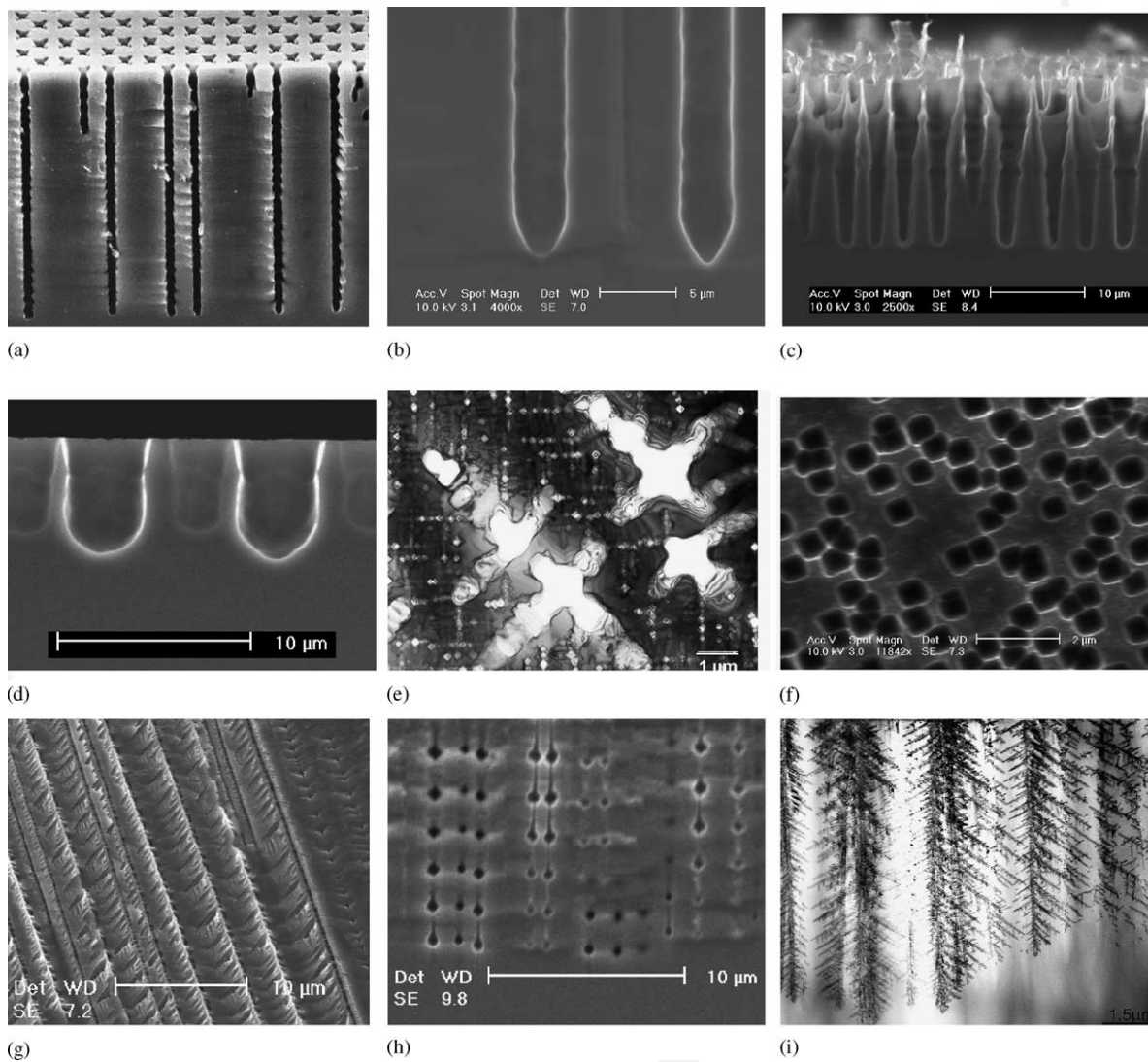


Fig. 2. Some examples demonstrating the variety of pores found in Si: (a) seeded n-macropores(aqu/bsi) from the first experiments performed [35], (b) random n-macropores(aqu/bsi) from [39], (c) n-macropores(aqu/fsi), (d) p-macropores(aqu), (e) n-macropores(org/bsi) as seen in pore growth direction by TEM, (f) n<sup>+</sup>-macropores(aqu + ox), (g) n-macropores(org/bsi), (h) n-macropores(org/bsi) with sin modulated current and non-linear response, (i) n-macropores(org/bsi).

148 “proper” mesopores as soon as their diameter exceeds 50 nm. “Break through” pores, e.g. obtained  
 149 in n-type Si in the dark at large potentials (and in all electrolytes), while very similar in appearance  
 150 to n<sup>+</sup>-mesopores(aqu), tend to be a bit larger in diameter and may exceed the 50 nm limit, but still  
 151 will be called n-mesopores(dark) in this paper.

152 It should be noted that current research produced “pores” that cannot be adequately described  
 153 in this system. Examples are the two-dimensional “trenches” and “wings” [22] observed under  
 154 conditions that also produce p-macropores(org) and n-macropores(org/bsi), respectively, cf. Figs. 6b  
 155 and 15b.

156 Why do pores form under a wide range of experimental conditions and what determines their  
 157 geometry and morphology? As stated before, the authors are of the opinion that pore formation



158 cannot be understood by itself, but must be seen in a larger context that includes the other salient  
159 features of the Si electrode. A first attempt at such a generalized model, including pore formation,  
160 has been proposed by the authors [10,12,20]; it attempts to describe all features of Si  
161 electrochemistry as the expression of the interaction between stochastically occurring “current  
162 bursts” (CB) which are localized in space and time. This model is called the current burst model  
163 (CBM) and will be briefly described in Section 7.

### 164 1.3. Pore formation models

165 It is not necessary to go into details of the various pore formation models in order to obtain  
166 some basic understanding of what determines pore parameters. No matter what kind of pores results  
167 from some experiment, they always have some characteristic dimensions—average diameter,  
168 average distance, spacing between branches—and all these length scales are usually rather well  
169 defined. While not many quantitative investigations on characteristic dimensions have been made, it  
170 is safe to say that pore formation of any kind (almost) always defines a specific length scale  
171 prevalent in the Si—electrolyte system employed that expresses itself in the (average) pore geometry  
172 and morphology. Any model thus must ultimately give a reason for the actual scale found in the  
173 pores under investigation in order to explain the geometry. Note, however, that the presence of a  
174 specific length scale does not necessarily explain pore formation per se.

175 The most advanced models for pore formation essentially give a reason for pore nucleation and  
176 stability and define a characteristic length scale. The most important length scales proposed are as  
177 follows.

- 179 • *Width of the space charge region ( $L_{SCR}$ )*. This was first proposed by Lehmann and Föll [35] not  
180 only as the major parameter governing pore geometry and morphology, but also as the only cause  
181 for the actual formation of n-macropores(aqu/bsi). The model has been quantified to some extent  
182 [36] and has been used with great success to produce beautiful pore structures for many  
183 applications [37,38]. However, while  $L_{SCR}$  and other effects due to the space charge region  
184 undoubtedly are very important for pore parameters, it has become obvious that  $L_{SCR}$  is not  
185 sufficient to explain macropores in general [39], not least because it relies heavily on the presence  
of a PSL-peak which is not observed for most org electrolytes.
- 187 • *Pore tip radius  $L_{AV}$  inducing avalanche break down*. At high field strengths at pore tips with a  
188 sufficiently small radius, avalanche break down necessarily occurs, supplying plenty of carriers to  
189 drive the electrochemical reactions—a process often exploited in n-type semiconductors where  
190 holes are scarce. While not a new idea [40], Lehmann et al. give a fully quantitative treatment and  
191 apply this effect to pore formation in general [41]. However, while avalanche break down will  
192 occur under certain conditions, it will be a locally and temporarily self-stopping process if some  
193 oxide formation occurs because this will locally decrease the field strength. Seen in this context,  
194  $L_{AV}$  will give the smallest dimensions possible for pores obtainable under conditions where it  
195 occurs. Smaller pores will simply grow to a diameter just above  $L_{AV}$  and avalanche break down  
196 only happens “every once in a while and here or there”—stochastically, in other words. In  
197 addition, the relative avoidance of avalanche break down will lead to round pore tips having a  
constant field strength at any point.
- 199 • *Diffusion instabilities*, well known from the growth of dendritic crystals (e.g. snowflakes) may  
200 induce gradients in the hole concentration with a typical dimension  $L_{DIF}$  and thus induce or  
201 stabilize pores with that dimension. This case was treated in detail by Chazalviel et al. [42], Smith  
and Collinsbut [43] since  $L_{DIF}$  is always tied to the diffusion length or Debye length of the holes,

202  $L_{\text{DIF}}$  is too restricted to account for all effects. It appears, however, that  $L_{\text{DIF}}$  is an important length  
203 scale for some p-macropore (org) systems.

- *Quantum wire effects* at length scales below  $L_{\text{qu}} \approx 1$  nm that prevent the movement of holes to the  
205 Si–electrolyte interface. This effect was invoked to explain the formation of micropores [44].  
206 However, while  $L_{\text{qu}}$  may define the minimum distance between micropores, it has nothing to say  
207 about the diameter of the micropores itself.
- Another typical length, often overlooked, is the *spacing between lithographically defined nuclei*,  
209  $L_{\text{NU}}$ , which is totally independent of the system parameters and thus a truly extrinsic length scale.
- The CBM finally defines a typical length scale, too, called the *correlation length*  $L_{\text{CO}}$  of the  
211 interaction between localized current bursts [12,20]; see Section 7 for details.

212

213 All these length scales definitely exist—at least in a subset of the available parameter space—  
214 and influence the geometry and morphology of pores. It is, however, not always clear which scales  
215 dominate the pore formation process and what will happen when major conflicts of length scales are  
216 unavoidable. For example, a clear conflict of scale occurs when the extrinsic length scale  $L_{\text{NU}}$  is too  
217 different from  $L_{\text{SC}}$ —it is simply not possible to obtain macropores spaced at distances much larger or  
218 much smaller than  $L_{\text{SC}}$ . Another conflict of scales occurs if one tries to produce macropores with  
219 diameters much smaller than  $L_{\text{AV}}$  or  $L_{\text{CO}}$ —and this is as much a prediction as a (largely unpublished)  
220 experimental fact.

221 It should be realized that there is a large body of experimental results that was never published,  
222 especially if the experiments were made with a particular goal in mind that could not be achieved.  
223 Etching well-formed macropores in the sub- $\mu\text{m}$  region, e.g. has been tried in several laboratories; but  
224 only one success was reported for a 0.5  $\mu\text{m}$  geometry after extensive work (including growing a  
225 special Si crystal) [45] while the unsuccessful attempts at even smaller spacings have not been  
226 published (including the efforts of the authors). Defined modulations of macropore diameters fall in  
227 this category, too.

## 228 2. Formation of macropores

### 229 2.1. Macropores in n-silicon obtained in aqueous electrolytes with back side illumination

230 Since n-macropores(aqu/bsi) are the best known species of macropores, we will consider them  
231 in some detail before treating the other kinds. “Perfect” pores with very large aspect ratios have  
232 been obtained for this species, and “perfect” means not only smooth pore walls, but also smooth  
233 cross-sections (albeit not necessarily circular) and constant diameter with depth.

234 The n-macropores(aqu/bsi) were first predicted by one of the authors and then found in a  
235 suitably designed experiment [35]. The prediction was based on results obtained in general  
236 electrochemical experiments with Si which produced precursors of n-macropores(aqu/fsi), cf.  
237 Fig. 13a). The basic idea was that the system n-Si/electrolyte is reversely biased in electrical terms,  
238 and that any bending of the prominent space charge region (SCR) in the Si by proto-pores would  
239 focus some of the holes produced by light on the pore tip. If holes would be available from the back  
240 side only, e.g. by back side illumination of samples with sufficiently large diffusion lengths for the  
241 minority carriers, they would be focussed by the SCR on the pore tips and macropores should grow  
242 with constant diameters to considerable depths.

243 Experiments were performed with lithographically defined nucleation (simply by using typical  
244 DRAM trench masks) and proved immediately successful, giving some weight to the simple “space

245 charge region pore formation model” (SCR-model) invoked. Further investigations and optimiza-  
 246 tions, mostly by Lehmann and coworkers (e.g. [36,38]), supplied some theoretical background and  
 247 developed this etching technology to a fine art.

248 In particular, Lehmann proposed a simple formula (“Lehmann’s formula”) that related the  
 249 cross-sectional area  $A_{\text{po}} \approx d^2$  ( $d$  = diameter of the pore) of the pore to the area  $A_{\text{cell}} = a^2$   
 250 ( $a$  = lattice constant) of a unit cell of the pore lattice and to the current density  $j$  via

$$\frac{A_{\text{cell}}}{A_{\text{po}}} = \left(\frac{d}{a}\right)^2 = \frac{j}{j_{\text{PSL}}} \quad (2.1)$$

253 with  $j_{\text{PSL}}$  = current density of the PSL-peak of the system (cf. Fig. 1). For “random” pores obtained  
 254 without predefined nucleation, or non cubic pore lattices, averages of  $d$  and  $a$  have to be taken. Since  
 255 the PSL-peak depends almost exclusively on the HF concentration and is thus a known quantity,  
 256 Lehmann’s formula is of considerable practical value.

257 The reasoning behind the formula is easy to understand: if stable macropores form and grow, all  
 258 current must flow through the macropores and the current density in a pore is then

$$j_{\text{pore}} = \frac{jA_{\text{cell}}}{A_{\text{po}}} \quad (2.2)$$

262 The pore thus has a “choice” of adjusting itself to an optimum current density by adjusting its  
 263 diameter, and  $j_{\text{PSL}}$  is a logical choice, being the only special current density in the characteristics  
 264 which, moreover, signifies the switch-over to electropolishing.

265 Obviously, Lehmann’s formula is only applicable to n-macropores(aqu/bsi) under conditions  
 266 where the applied potential is significantly larger than  $U_{\text{PSL}}$ , the potential corresponding to the  $j_{\text{PSL}}$ -peak,  
 267 and perhaps to some extent to n-macropores(fsi), but not to p-macropores(aqu), and especially not to p,  
 268 n-macropores(org), because the relevant  $I(V)$ -characteristics do not contain a PSL-peak.

269 Eq. (2.1) would allow any pitch  $d/a$ , i.e. arbitrarily large or small pores at any spacing. This is  
 270 not realistic, however, because the basic premises of the SCR-model was that the space charge region  
 271 must be bend around a pore but not penetrate between the pores. This imposes somewhat fuzzy  
 272 limits on  $d$  and  $a$ : it must be expected that stable pore growth is only possible if  $d$  and  $a$  are in the  
 273 same order of magnitude as  $L_{\text{SCR}}$ , the width of the space charge region. This is illustrated in Fig. 3.

274 The validity of Lehmann’s formula is demonstrated in a series of experiments where the  
 275 distance  $a$  between pores was varied between 4 and 64  $\mu\text{m}$  while the pitch  $d/a$  was kept constant;  
 276 some results are shown in Fig. 4.

277 It can be seen that if  $a$  is too small, some pores stop to grow, and if  $a$  is too large, the pore  
 278 surfaces become rough and that the diameters are smaller than expected. While Grüning et al.  
 279 showed that there is still preferred carrier flow to the pore tips even for spacings larger than  $2 L_{\text{SCR}}$   
 280 [46], there is, however, still stable pore growth at distances where carriers can easily penetrate the  
 281 area between the pores (corresponding to Fig. 3b) which gives a definite indication that something  
 282 else besides the diversion of carriers to pore tips by the SCR must stabilize pore walls against further  
 283 dissolution. Contrariwise, it is not clear from the SCR-model alone, why case (d) in Fig. 3—making  
 284 very thin pores at a relatively large spacing—is apparently not possible.

285 It is thus not easily possible to produce n-macropore(aqu/bsi) arrays with  $d \gg 1 \mu\text{m}$ , or  
 286  $a \gg 5 \mu\text{m}$  with standard Si samples. Noteworthy exceptions are the photonic crystals produced with  
 287 n-macropore(aqu/bsi) arrays at dimensions of  $0.5 \mu\text{m}$  [45] using a specially grown Si crystal (FZ,  
 288 highly doped but still with a large diffusion length of minority carriers), and, at the other extreme,  
 289 pore arrays with  $>100 \mu\text{m}$  dimensions [47].  
 290



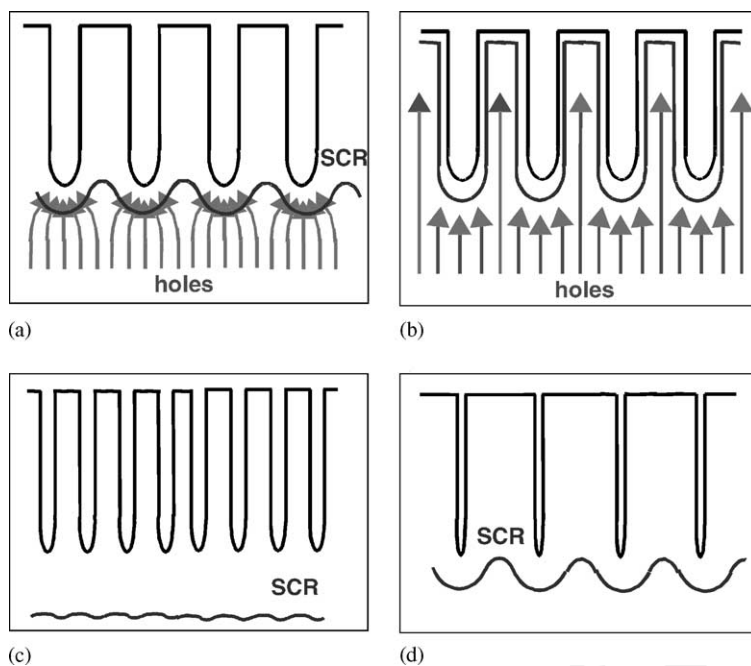


Fig. 3. Four basic cases of SCR controlled n-macropore(aqu/bsi) growth: (a) space charge region width  $L_{SCR}$  matched to  $a$ ; (b)  $a \gg L_{SCR}$ ; (c)  $a \ll L_{SCR}$ ; (d)  $a \approx L_{SCR}$ ,  $d \ll L_{SCR}$ .

291 From these considerations a few more inferences can be made with respect to achievable pore  
 292 geometries.

- Without extrinsically defined pore nucleation, “random” pores will result and their average  
 294 diameter  $\langle d \rangle$  and spacing  $\langle a \rangle$  can be expected to be comparable to  $L_{SCR}$ . One study of this topic

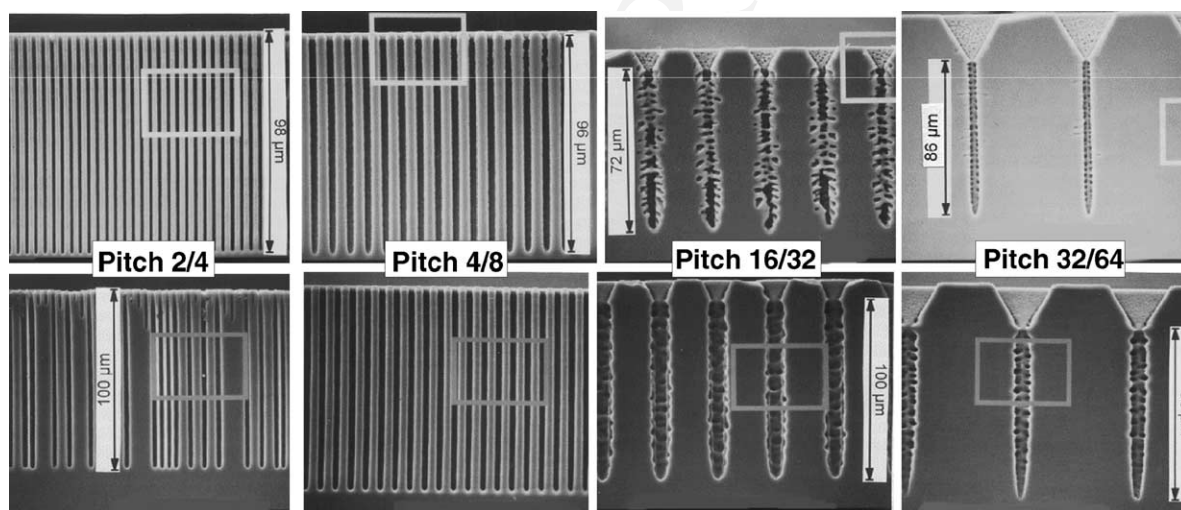


Fig. 4. The n-macropores(bsi) etched in 4% HF solution at 2 V with pre-structured nuclei at variable distances from 4 to 64  $\mu\text{m}$  and etching currents and times adjusted to yield constant pitch and depth. Upper row: 5  $\Omega\text{ cm}$  ( $L_{SCR} \approx 1\ \mu\text{m}$ ), lower row 40  $\Omega\text{ cm}$  ( $L_{SCR} \approx 3\ \mu\text{m}$ ) Si samples.

295 has been made [39] and while the general prediction is correct, there are clear exceptions for  
296 highly doped Si.

• Etching n-macropores(aqu/bsi) in defined areas only, with the help of, e.g. a  $\text{Si}_3\text{N}_4$  mask, has been  
298 tried repeatedly, but unsuccessfully. While macropore arrays with good quality could be obtained  
299 in the interior of the unmasked area, there will always be some macropore growth under the  
300 mask—in rather irregular fashion. This indicates that whatever mechanism protects the pore walls  
301 from etch attack under conditions as, e.g. shown in Fig. 4 for large lattice constants  $a$ , is not  
302 sufficiently strong under the pertaining conditions to keep the walls totally inert. While it is too  
303 early to say that this task (which is of obvious technical importance) can never be achieved, it is  
304 probably safe to say that the pore etching and pore wall passivation mechanisms must be much  
305 better understood for a successful solution of this practical problem.

• Intentionally introduced defects in regular arrays (e.g. missing pores) are possible, as long as the  
307 distances between the remaining pores do not become too large. The pores next to the defects will  
308 then increase their diameter slightly to accommodate the surplus holes. It is not possible, however,  
309 to produce isolated pores because the many holes not flowing to the pore tip will eventually either  
310 induce random nucleation of pores, or erode the pore walls of single pores, or both.

• The pore diameter cannot be adjusted for individual pores, but only for the pore assembly by varying  
312 the etching current during etching. As long as the chemical processes are fast enough, the diameter  
313 as a function of depth  $z$  should follow the current modulations in time, or  $d(z) = vj(t)$  with  
314  $v =$  growth velocity of the pores. Inducing controlled diameter modulations, however, has proved to  
315 be surprisingly difficult. While it is possible in principal [48], it is often observed that  $d(z)$  does not  
316 follow  $j(z)$  but reacts rather non-linearly to current modulations as illustrated in Fig. 2h.

• While Lehmann's formula should apply to all HF concentrations (which essentially define  $j_{\text{PSL}}$ ),  
318 the general experience is that it is very difficult if not impossible to obtain smooth n-  
319 macropores(aqu/bsi) for HF concentrations above about 10%. This severely limits the growth rate  
320  $v$  for n-macropores(aqu/bsi) to (rule of thumb)  $\approx 1 \mu\text{m}/\text{min}$ .

• For very smooth pores and large aspect ratios, all etching parameters have to be “just right”. This  
322 includes the HF concentration, the voltage, the temperature, and the flow of the electrolyte.  
323 Changing one parameter without properly readjusting the others will tend to result in less perfect  
324 pores.

• For deep pores, diffusion effects have to be taken into account. The diffusion of molecules into  
326 and out of the pores becomes more difficult as the pore depth increases, while the diffusion of  
327 holes to the pore tip becomes easier as the distance between the pore tip and the illuminated  
328 backside decreases. Both effects change  $j$  and  $j_{\text{PSL}}$ , so simply keeping  $j =$  constant during an  
329 etching experiment will not necessarily keep the pore diameters constant. Lehmann analyzed these  
330 effects in detail [36] and developed a software that compensates for the chemical diffusion effects  
331 during etching taking into account also the temperature dependence of the processes. Several  
332 groups active in the field use this software and thus automatically obtain the geometric parameters  
333 independent of temperature and diffusion—in principle. There are, however, still pronounced  
334 effects, particularly with respect to the etching temperature (cf. [9]), that are not included in the  
335 software (or not even understood).

• It may be useful in certain instances, to over-etch the n-macropores(aqu/bsi) by a (usually very  
337 gentle) purely chemical etch. This will enlarge the pore diameters and smooth the walls if done right.  
338

339 One more interesting point concerning n-macropores(aqu/bsi) is the dependence of the pore  
340 morphology on the sample orientation. Most models are silent on this point (they would be fully  
341 applicable to amorphous semiconductors, too); the expectation at best would be that pores grow

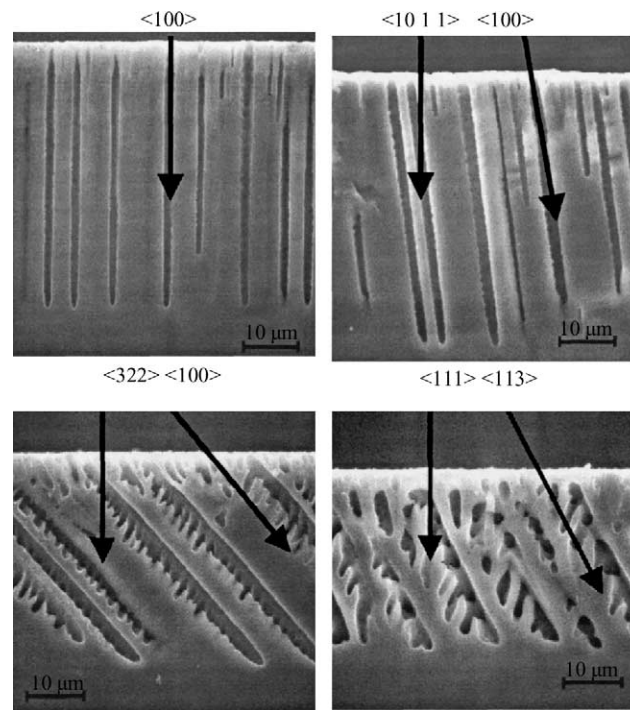


Fig. 5. Orientation dependence of (random) n-macropores(aqu/bsi). The substrate orientation is (a)  $\langle 1 \ 0 \ 0 \rangle$ , (b)  $\langle 10, 1, 1 \rangle$ , (c)  $\langle 3 \ 2 \ 2 \rangle$ , and (d)  $\langle 1 \ 1 \ 1 \rangle$ . In (d)  $\langle 1 \ 1 \ 3 \rangle$  oriented pore tripods result.

342 directly towards the source of the holes, i.e. perpendicular to any surface. This is decidedly not the  
 343 case. Detailed investigations [21] showed that n-macropores(aqu/bsi) grow exclusively in  $\langle 1 \ 0 \ 0 \rangle$   
 344 directions and (occasionally, if all available  $\langle 1 \ 0 \ 0 \rangle$  directions are steeply inclined) in  $\langle 1 \ 1 \ 3 \rangle$   
 345 directions. Their morphology is always describable as a main pore in one of this two directions and side  
 346 pores or branches in some of the others. Fig. 5 shows some examples. This fact, again, demonstrates  
 347 drastically that the SCR-model alone cannot account for all n-macropore(aqu/bsi) features.

348 The dependence of the pore morphology on sample orientation is just as complex for other  
 349 kinds of pores, too; it will be covered in the appropriate sections. Whereas not many practical uses  
 350 for the peculiarities of orientation dependence have been envisioned so far (for an exception, see  
 351 Section 3), some more ideas are emerging. In any case, orientation dependence of pore growth is a  
 352 major issue for modeling purposes and thus may be beneficial for applications in an indirect way.

353 In total, producing arrays of “perfect” n-macropores(aqu/bsi) with defined dimensions and  
 354 possibly including defects (e.g. for photonic crystals), while easy in principle, requires carefully  
 355 designed experiments with plenty of fine tuning, even on the laboratory scale (with typical sample  
 356 dimensions of a few  $\text{cm}^2$ ). Etching n-macropores(aqu/bsi) in standard Si wafers of at least 100 mm,  
 357 possibly 300 mm diameter, requires a major investment (in time and money) into the construction of  
 358 a suitable apparatus. So far, few groups have attempted this, but it can be done as shown by Lehmann  
 359 and Grüning [38] and van den Meerakker et al. [49]. We will come back to this point in Section 6.

## 360 2.2. Other types of macropores and related structures

361 The n-macropores(aqu/bsi) have been targeted for a number of applications and several projects  
 362 are under way towards a commercial product; this will be covered in Section 3. This is not (yet) the

Table 1  
Comprehensive listing of macropore types and two-dimensional structures observed so far

Type	Remarks
n-Macropores(aqu/bsi)	Oldest and “best” types of macropores, “Lehmans formula” applies, SCR limits distances; diameter limitation uncertain but diameters $< 0.8 \mu\text{m}$ difficult to obtain. Maximum depth $> 600 \mu\text{m}$ achieved. Obtained for $j < j_{\text{PSL}}$ ; but no “good” pores for $[\text{HF}] > 10\%$ ; $U > 5 \text{ V}$ . Temperature is important
n-Macropores(aqu/fsi)	Not much investigated
n-Macropores(org/bsi)	Only investigated for DMF/4% HF. “Strange” morphologies, mix with mesopores, peculiar growth dynamics
p-Macropores(aqu)	Observed for “low” currents and HF concentrations (otherwise micropores result), potentially useful because relatively easy to make
p <sup>+</sup> -Macropores(aqu + ox)	Only known exception to the rule that only mesopores form in highly doped Si. Potentially useful for small diameters
p-Macropores(org)	Large range of macropores observed, from shallow depressions to macropores rivaling the best n-macropores(bsi). Decisive parameters are electrolyte conductivity, “oxidizing power”, “passivation power” and dielectric constant. Large potential for applications because SCR restrictions are less severe
Secondary macropores	Long nucleation phase, always filled with mesopores
p-Trenches(org/masked)	Two-dimensional trenches instead of macropores may result if a $\text{Si}_3\text{N}_4$ mask is used to define areas to be etched
n-Wings(org/bsi)	Two-dimensional cavities bound by $\{111\}$ planes on the upper side may occur, with n-macropores(org/bsi) hanging down like stalagmites

363 case for the other types of macropores—they are too new for that. However, n-macropore(aqu/bsi)  
 364 technology is not only rather difficult (requiring backside illumination) but has several limitations  
 365 that the other macropore types may or may not have. We will therefore cover these new  
 366 developments in some detail, too.

367 As already mentioned, macropores now can be made in a variety of very different ways, Table 1  
 368 gives a short overview together with the more outstanding features.

369 Some entries, suggested by symmetry, are missing. Only first experiments on n-macropores(org/  
 370 fsi) exist (cf. Figs. 13 and 26d), while n<sup>+</sup>-macropores(aqu + ox) seem not to exist; a search for them  
 371 has been made but was not successful—mesopores were obtained under all conditions tried [34].

372 The entry “secondary macropores” needs an explanation. This kind of macropores forms if  
 373 mesopores (or possibly micropores) are formed as the primary pores (responding to a small primary  
 374 length scale of the system) while a large secondary length scale eventually causes an instability of  
 375 the pore front. Bulgy secondary macropores filled with mesopores may result, e.g. because of  
 376 diffusion instabilities; cf. Fig. 7f).

377 Besides (macro)pores—always defining an one-dimensional structure with a length in  $z$ -  
 378 direction (potentially) much larger than its lateral  $x$ - and  $y$ -dimensions—two-dimensional structures  
 379 have been observed recently that occur in close connection with macropores [50]. The first of these  
 380 new etching features is obtained if p-macropore(org) etching is tried in defined areas only, the rest  
 381 being protected by a  $\text{Si}_3\text{N}_4$  mask (without a buffer oxide as commonly used in microelectronics).  
 382 Depending on the etching conditions and in particular on the nitride thickness, a trench (or fissure)  
 383 along the mask edge is observed that penetrates much deeper into the Si than the p-macropores(org)  
 384 in the inside of the open area. Fig. 6 gives an example, for details see [50]. In what follows we use  
 385 the name *trench* for this structure which should not be confused with the “trenches” in integrated  
 386 circuits (DRAMs; the microelectronic community calls holes or pores “trenches” (as in “trench”  
 387 capacitor) for rather obscure reasons) or with the “trenches” to which some older pore literature  
 388 referred on occasion (e.g. the first n-macropore(aqu/bsi) paper [35]), when pores were meant.  
 389 Trenches have obvious potential uses; this will be discussed later.

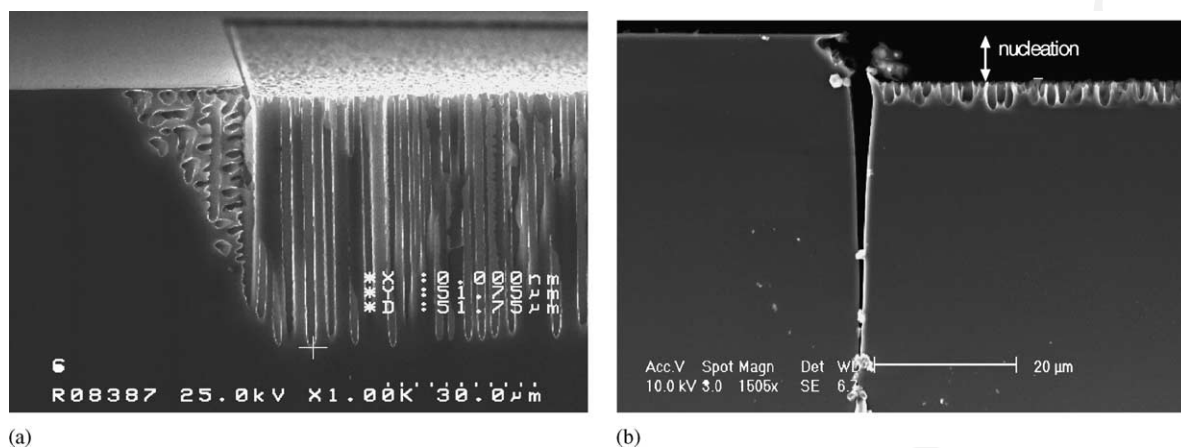


Fig. 6. (a) Regular p-macropores(org/DMF), showing under-etching of the nitride mask. (b) A “trench” running along the mask etch together with shallow p-macropores(org/DMF) obtained under similar conditions.

390 A second two-dimensional etching structure (“wings” [51]) was found in connection with  
 391 n-macropores(org/bsi) and will be treated there.

### 392 2.3. Macropores in p-silicon obtained in organic electrolytes

393 The first p-macropores(org) were found by Propst and Kohl in 1994 [33]. In the following years,  
 394 many papers have been published dealing with new kinds of p-macropores(org) obtained by using  
 395 different kinds of organic electrolytes, e.g. [52–56]. While it first appeared that p-macropores(org)  
 396 were limited to Si with a rather high resistivity of  $\geq 100 \Omega \text{ cm}$  (resulting in relatively short and  
 397 “bulgy” pores), Ponomarev and Levy-Clement [53] were the first to etch macropores on  $1 \Omega \text{ cm}$   
 398 (1 0 0) and (1 1 1) orientated Si substrates using different organic electrolytes. Christophersen et al.  
 399 finally found very stable growth conditions for p-type macropores (org) allowing for pore depths up  
 400 to  $400 \mu\text{m}$  [54]. Fig. 7 gives a sample of the kinds of p-macropores(org) that could be obtained so far.

401 This situation was (and is) somewhat puzzling, because the SCR-model generally used to  
 402 explain n-macropore(aqu) formation did not seem to allow for macropore formation in p-type Si at  
 403 all. The avoidance of holes between the pore walls with the bsi—“trick” is not possible, the space  
 404 charge region can never be very wide, and thus should have much less “focussing” power.

405 The p-macropores(org) may be coming close to applications. Ohji et al. were able to build free  
 406 standing silicon structures based on electrochemically etched p-macropores(org) using pre-  
 407 structured p-type silicon [55], while Chao et al. presented deep p-macropores(org) with depths up  
 408 to  $400 \mu\text{m}$  and found that pre-structuring significantly stabilized pore growth [56]. Possible  
 409 advantages in comparison with n-macropores(aqu) are a somewhat simpler cell design (no backside  
 410 illumination necessary) and (so far) unknown limitations—maybe etching speeds could be higher, or  
 411 pores with a smaller pitch are possible? On the other hand, the electrolytes are often very aggressive  
 412 (only polyfluorated materials might be usable for the electrochemical cell) and expensive to get rid  
 413 of in an orderly fashion.

414 We may consider two deep questions in connection with p-macropores(org)—one more  
 415 fundamental, one more practical.

416 1. What are the mechanisms responsible for formation of p-macropores(org) and which parameters  
 417 determine geometry and morphology?



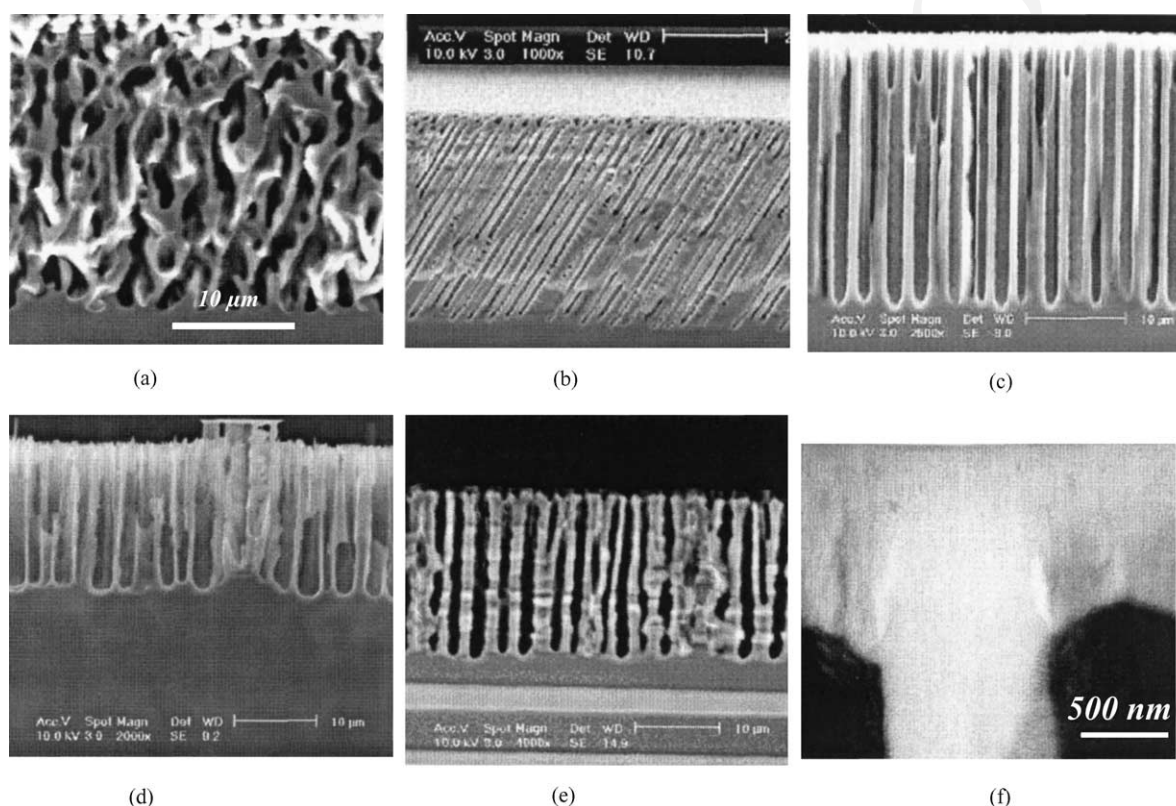


Fig. 7. Some samples of p-macropores(org) with 4 wt.% HF: (a) MeCN, {1 1 1} sample; (b) DMF on {5 1 1} Si; (c) DMF—perfect pores; (d) HMPA; low current density—bulgy pores; (e) MeCN + diethyleneglycol (protic additive); (f) TEM of secondary pore formation on {1 0 0}.

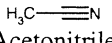
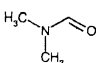
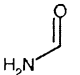
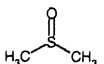
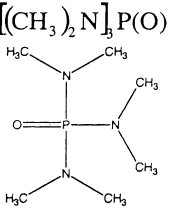
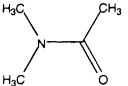
418 2. Given the inexhaustible (chemical) parameter space, how do we find optimized etching  
 419 conditions for a particular task, i.e. electrolyte composition, current density, voltage, and  
 420 temperature?  
 421

422 Exhaustive answers to these questions are not yet in. We will try to give partial answers by  
 423 listing some generalized points extracted from a host of experiments with p-macro-pores(org), and  
 424 by some speculations based on the CBM. First, however, the major organic compounds used so far  
 425 are listed with some of their properties in Table 2. The numbers in the entry “oxidizing power” give  
 426 the slope of the  $U(t)$  curves obtained for anodic oxide formation with a constant current density as  
 427 discussed before.

428 The HF addition is always 4% HF by weight if not otherwise stated. Since the HF is usually  
 429 taken from a standard 49% HF solution, organic electrolytes therefore will always contain some  
 430 water coming from the HF. Exceptions are the studies reported in [33] where essentially no direct  
 431 macropores were found but, as far as indicated, only “second order” macropores according to our  
 432 nomenclature (and expectation).

433 So far, there are no clear and simple rules for the pore geometry comparable to “Lehmann’s  
 434 formula” for n-macropores(org). At present, the work of Chazalviel et al. [42], considering mostly  
 435 diffusion instabilities, may come closest to making some predictions, especially for the case of low  
 436 doped (and amorphous) Si. A few general points are as follows.

Table 2  
Organic electrolytes used in Si electrochemistry and some of their major properties

Symbol	Formula name	Polarity (DK)	Oxidizing power
MeCN	 Acetonitrile	6.2	Very weak; slope of anodic oxide, 0 a.u.
DMF	 Dimethylformamide	6.4	Slightly oxidizing, 0.5 a.u.
FA	 Formamide	7.3	Strong, 3.5 a.u.
DMSO	 Dimethylsulfoxide	6.5	Mild oxidizing, 2.5 a.u.
HMPA	$[(\text{CH}_3)_2\text{N}]_3\text{P}(\text{O})$  Hexamethylphosphoric triamide	6.6	Oxidizing, 6.5 a.u.
DMA	 Dimethylacetamide	6.3	Mild oxidizing, 2.1 a.u.

- 438 • The doping of the Si is rather important. Increasing the doping level acts to some extent like  
439 increasing the applied potential. In general, high doping levels reduce the ability to form  
440 macropores [34,57]. Viewed relative to aqueous electrolytes, the switch-over to mesopores occurs  
already at lower doping levels.
- 442 • The p-macropores(org) tend to become more “perfect” if the oxidizing power of the electrolyte is  
443 not too small (at least 0.5 on our scale). Electrolytes with little oxidizing power as, e.g. MeCN,  
444 will hardly produce macropores at all, whereas electrolytes with strong oxidizing power (e.g. FA,  
comparable to H<sub>2</sub>O or stronger) produce micropores instead of macropores.
- 446 • Stable growth to considerable depth also requires the availability of H or more precisely, it is  
447 related to the “passivation power” of the electrolyte in the context of the CB model. “Passivation  
448 power”, like oxidizing power, is not a property of standard chemistry but has nonetheless a well  
449 defined meaning: it denotes the degree to which a given electrolyte can remove interface states in  
450 the band-gap of Si by covering a freshly etched surface with hydrogen. This is a measurable  
451 quantity in principle, but while preliminary measurements based on the ELYMAT technique [15]  
452 have been made, no reliable data exist at present. The following remarks are either based on  
453 circumstantial evidence or may be taken as predictions. It is therefore of importance whether the  
electrolyte is protic or aprotic (i.e. donates or accepts hydrogen) and, of course, the pH value may

454 be involved [58], but might not always be of prime importance [14]. In the CBM, H-passivation is  
 455 the major process responsible for pore formation and it has been shown that additions of protic  
 456 substances to an org-electrolyte change the pore growth in the expected way [22].

- The dielectric constant (DK) of the electrolyte must be considered. Essentially, the DK determines to which degree HF will be fully dissociated and thus “active”. Electrolytes with a low DK tend to have a reduced HF “activity” which slows down the direct dissolution process and the oxide dissolution.

- The conductivity of the electrolyte is of course of considerable importance, too. It would be too naive to assume that the resistance of the electrolyte can be easily compensated for by increasing the voltage, because diffusion of species in the electrolyte can lead to phenomena similar to the diffusion of holes in the semiconductor and therefore introduce instabilities that cause, modify or interfere with pore formation, cf. [42,59].

- Temperature, circulation of the electrolyte, small additions of surfaces reactant, or bubbling with  $N_2$  to remove oxygen dissolved from the air, may also be of importance.

- The nucleation of p-macropores(org) can be achieved by supplying pre-structured nuclei as in the case of n-macropores(bsi), but not many investigations have used this technique (see [36] for example). Homogeneous random nucleation, on the other hand, can be rather difficult and may only occur after a certain period of larger voltages intentionally supplied for the nucleation phase or automatically employed by the potentiostat if galvanic conditions are used, cf. Fig. 8.

- The orientation dependence of p-macropores(org) is similar to that of n-macropore(aqu), but often not quite as pronounced because the pores are often not well defined (cf. Fig. 7a).

- While the limitations with respect to pore geometries and morphologies are not known at present, recent experiments of the authors (following the guide lines from above and some rules derived from the CBM and published here for the first time) demonstrate that  $(0.2 \mu\text{m} \times 0.4 \mu\text{m})/0.2 \mu\text{m}$  pitches are possible (Fig. 9)—a feat are often tried, but never achieved with n-macropores(bsi). The pores have rough walls, demonstrating the need of fine tuning any process that is to deliver “perfect” pores.

480

481 The listing above contains implicit claims with respect to certain electrolyte properties, derived  
 482 from generalizations of measurements as shown in Fig. 10. More data concerning the correlation of  
 483 p-macropores(org) and properties of the chemicals employed can be found in [22]. In essence, while  
 484 these investigation stress the traditional chemical point of view and provide valuable data concerning  
 485 the dependence of pore geometry and morphology on chemical properties and the conductivity of the

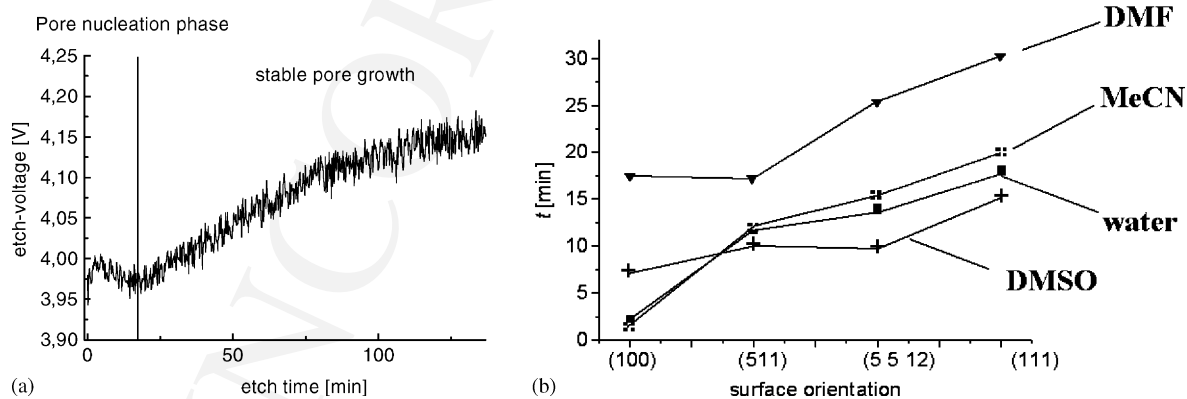


Fig. 8. (a) Development of the voltage over time for constant current and a DMF electrolyte. A nucleation phase, and a stable growth phase can always be identified. (b) Nucleation time for various electrolytes and surface orientations.

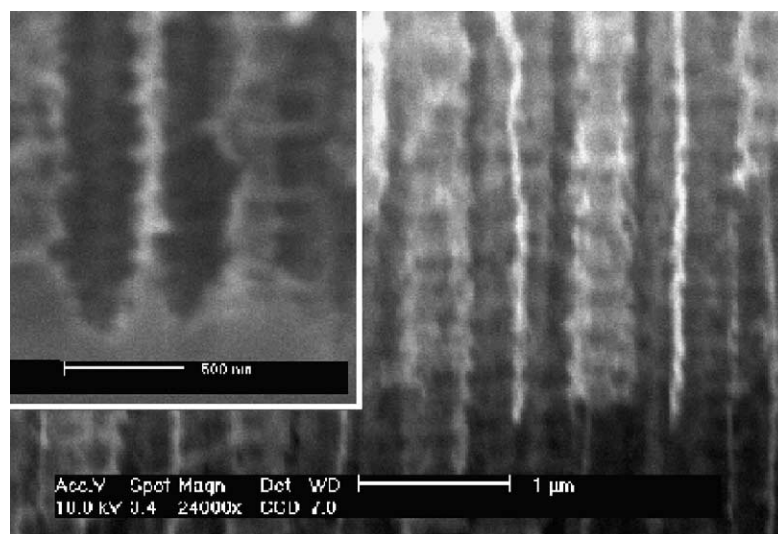


Fig. 9. First 200 nm macropores obtained by optimized organic electrolytes and etching conditions (the smallest pitch is perpendicular to the cleavage plane).

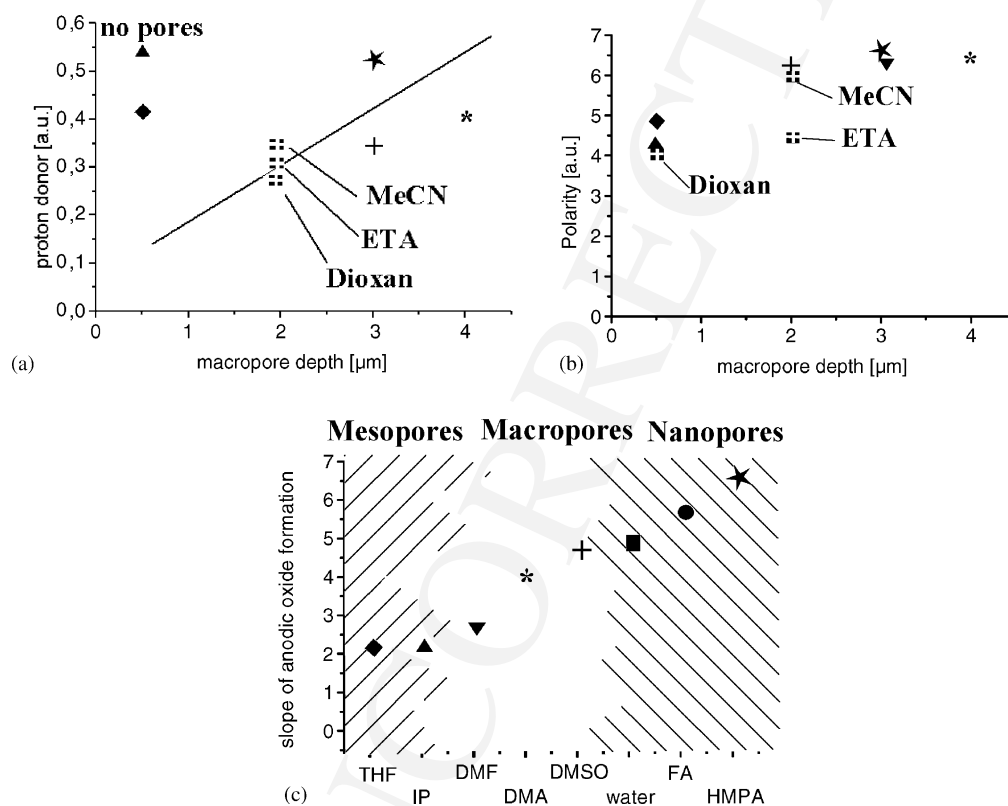


Fig. 10. Various correlations between p-macropore(org) properties and electrolyte properties. (a) Dependence of p-macropore(org) depth on the ability to donate protons of the electrolytes. The numbers are from [61]; the symbols were defined in Fig. 8b. (b) Polarity of organic electrolytes. It simply scales with the value of the dielectric constant or index of refraction. (c) Correlation of the oxidizing power and pore formation for various organic electrolytes (and H<sub>2</sub>O for comparison).

486 Si, little information can be deduced with respect to the questions at the outset of this paragraphs  
487 from standard chemistry alone.

488 In this context, it is important to point out again formamide (FA), a new kind of org electrolyte  
489 with an oxidizing power exceeding that of water and used here for the first time. FA electrolytes do  
490 not produce p-macropores(org), but p-micropores(org) (cf. Fig. 26), exhibit a PSL-peak in the  $I(V)$   
491 characteristics (cf. Fig. 1c) and current oscillations at high potentials, exactly as expected by the  
492 CBM (cf. Section 7).

493 Since the oxidizing power of the org electrolytes is so important, it is often necessary to bubble  
494 the electrolyte with  $N_2$  before use, in order to remove all traces of  $O_2$  dissolved from the air. Of all  
495 electrolytes tried, DMSO and DMA produce the most perfect p-macropores(org). There is little  
496 doubt that their combination of relatively large oxidizing power and sufficient passivation power  
497 supplies the best compromise for etching well-formed p-macropores(org).

#### 498 2.4. Macropores in p-silicon obtained with aqueous electrolytes

499 If p-macropores(org) came as a surprise, so did p-macropores(aqu) which were first described  
500 by Lehmann and Rönnebeck [60]—after several hundred papers had been published exclusively  
501 finding p-micropores(aqu). However, microporous Si is usually produced with electrolytes  
502 containing a large concentration of HF (often just 49% HF mixed with an equal volume of  
503 ethanol), and at current densities close to the  $j_{PSL}$  value of the system, while p-macropores(aqu) are  
504 found at current densities much lower than  $j_{PSL}$  and for medium to low HF concentrations. Fig. 11  
505 shows some representative species.

506 The p-macropores(aqu) occupy some region in the parameter space (roughly) defined by the HF  
507 concentration [HF] and the current density. While there is a general agreement in the literature that  
508 [HF] determines  $j_{PSL}$  (although, no doubt, the nature of the additions will play a minor role, too),  
509 there are few and seemingly contradictive quantitative data. Lehmann [36] reported an exponential  
510 relationship of  $j_{PSL}$  on [HF], while van den Meerakker et al. [49] found a linear dependence. The  
511 actual data, however, if plotted in the same diagram, are reconcilable as shown in Fig. 12. The figure  
512 also contains some predictions from the CB model as to the parameter space of p-macropores(aqu).

513 The SCR-model may account for these pores to some extent, because they occur at small  
514 currents which means that there is still a sizeable SCR that could focus carriers on pore tips and that  
515 would provide an impenetrable barrier for holes if the walls between p-macropores(aqu) are  
516 completely contained in the SCR [60]. Likewise, diffusion instabilities may favor p-macropores(aqu)  
517 to some extent.

518 Not many properties of p-macropores(aqu) are known at present; nevertheless, we attempt to  
519 summarize and generalize as follows.

- The p-macropores(aqu) are rather easily obtained for [HF] < 15 wt.% and  $j < 0.05j_{PSL}$  if  
521 nucleation is provided for, e.g. by KOH etch pits.
- Without pre-defined nucleation, an extensive nucleation period may be necessary.
- The walls between p-macropores(aqu) are always rather thin (corresponding to twice the SCR  
524 width).
- Lehmann's formula does not apply: there is no defined relation between  $a$ ,  $d$ , and other variables;  
526 pores with predefined nucleation always grow in diameter until they almost touch each other.
- Pores with large diameters obtained in this way, tend to have “cloudy” tip shapes, cf. Fig. 11b.
- Randomly nucleated p-macropores(aqu), while still keeping pore wall dimensions small, have  
529 well defined average diameters with smooth tips and walls (cf. Fig. 11a).



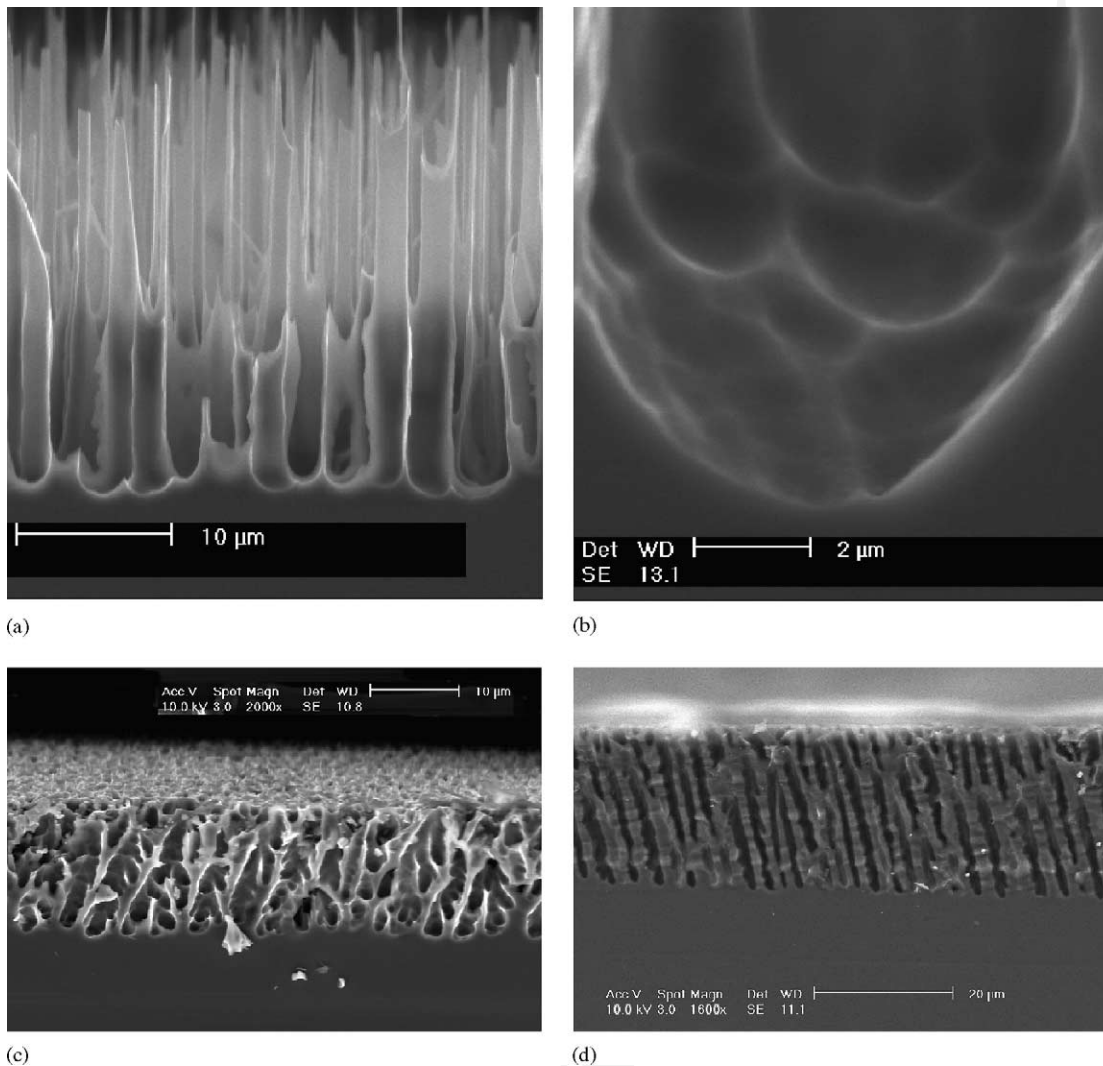


Fig. 11. Some samples of p-macropores(aqu): (a)  $10 \Omega \text{ cm}$ ; 7% HF,  $j = 20 \text{ mA/cm}^2$ ,  $j_{\text{PSL}} = 90 \text{ mA/cm}^2$ , random nucleation; (b) as (a), but induced nucleation (hexagonal lattice,  $a = 3 \mu\text{m}$ ); (c)  $10 \Omega \text{ cm}$ ; 10% HF,  $j = 2 \text{ mA/cm}^2 = 0$ ,  $j_{\text{PSL}} = 150 \text{ mA/cm}^2$ , random nucleation on {5, 5, 12} sample; (d) p-macropores(org) with MeCN (4 wt.% HF) on {1 1 1} for comparison with (c).

- Not much is known about the orientation dependence of p-macropores(aqu); but it appears to be similar to that of p-macropores(org) obtained from electrolytes with small oxidizing power. In particular, p-macropores(aqu) obtained in {1 1 1} Si, are practically indistinguishable from p-macropores(org) with MeCN as electrolyte—cf. Fig. 7c and d.
- The CBM predicts that p-macropores(aqu) occur for currents below the point of inflection on the  $I(V)$  characteristics [11].

The CBM has much more to say to the formation of p-macropores(aqu), but since so far no immediate uses have emerged, we will not dwell on the subject and mention it only briefly in Section 7.

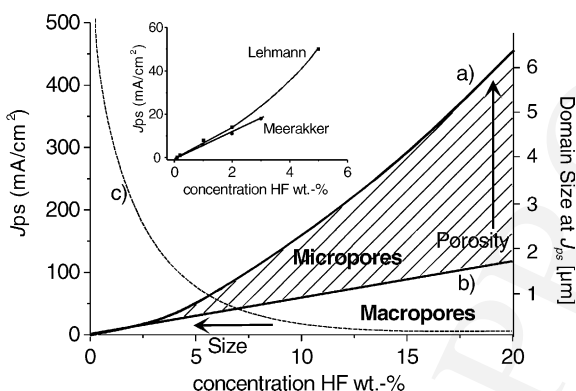


Fig. 12. Parameter space for p-micropores(aqu) and p-macropores(aqu). Curve (a) shows  $j_{PSL}$  as described by the Lehman model [36] and curve (b) as described by van den Meerakker [49]. Curve (c) describes the size of a CB domain. The regions for macropore- and micropore-growth are a result of a semiquantitative consideration of the CB model and may be considered as a prediction. The inset shows measured data taken from [36,49] for low HF concentrations.

#### 540 2.5. Macropores in n-silicon obtained in aqueous electrolytes using front side illumination

541 As in the case of p-macropores(aqu), the SCR-model would not necessarily expect well formed  
 542 macropores if the front surface of n-type Si is illuminated. As mentioned before, n-macropores(aqu/  
 543 bsi) were actually predicted based on observations with front side illumination; Fig. 13 includes  
 544 these “historical” pictures. Essentially, only conical depressions were obtained that would not be  
 545 called macropores [17].

546 Besides a systematic study of Levy-Clement et al. which established the existence of n-  
 547 macropores(aqu/fsi) [57], nothing else seems to be published about this kind of macropores. In  
 548 general, three different zones were found [24]: an etch crater, a microporous and a macroporous  
 549 silicon layer. The morphology of the zones depends strongly on the etch conditions, e.g. charge  
 550 transferred, doping level, HF concentration, surface orientation. The authors summarized that some  
 551 of their results are consistent with a depletion layer model while others are not.

552 Meanwhile, however, new results have been obtained published here for the first time and  
 553 shown in Fig. 13c and d. Well developed n-macropores(aqu/fsi) oriented in  $\langle 100 \rangle$ . A totally new  
 554 result is the observation of n-macropores(org/fsi), similar to the ones obtained in aqueous  
 555 electrolytes, but with stronger (periodic) branching. The inclined n-macropores(aqu/fsi) shown in  
 556 Fig. 13f serve to rule out that light penetrating a pore generates carriers at the pore tip and thus  
 557 promotes pore growth. Considering that a pore is the opposite of a wave guide and will quickly  
 558 scatter light into the Si, it is unlikely that carriers are generated close to the pore tip. The unavoidable  
 559 conclusion is that carriers must diffuse from the surface near region where they are generated to the  
 560 pore tips. While the conical shapes indicate that there is some initial lateral pore growth (especially  
 561 in the form of branches) in surface near regions, the strong unbranched growth in the depth  
 562 unambiguously requires some kind of passivation of the pore walls, as concluded in other cases  
 563 before.

#### 564 2.6. Macropores in $n^+$ -silicon obtained in aqueous electrolytes with additions of 565 oxidizing electrolytes

566 The  $n^+$ -macropores(aqu + ox) merit special mentioning (despite their present uselessness) for  
 567 two reasons: first, they demonstrate that there is still room for new findings within the context of the

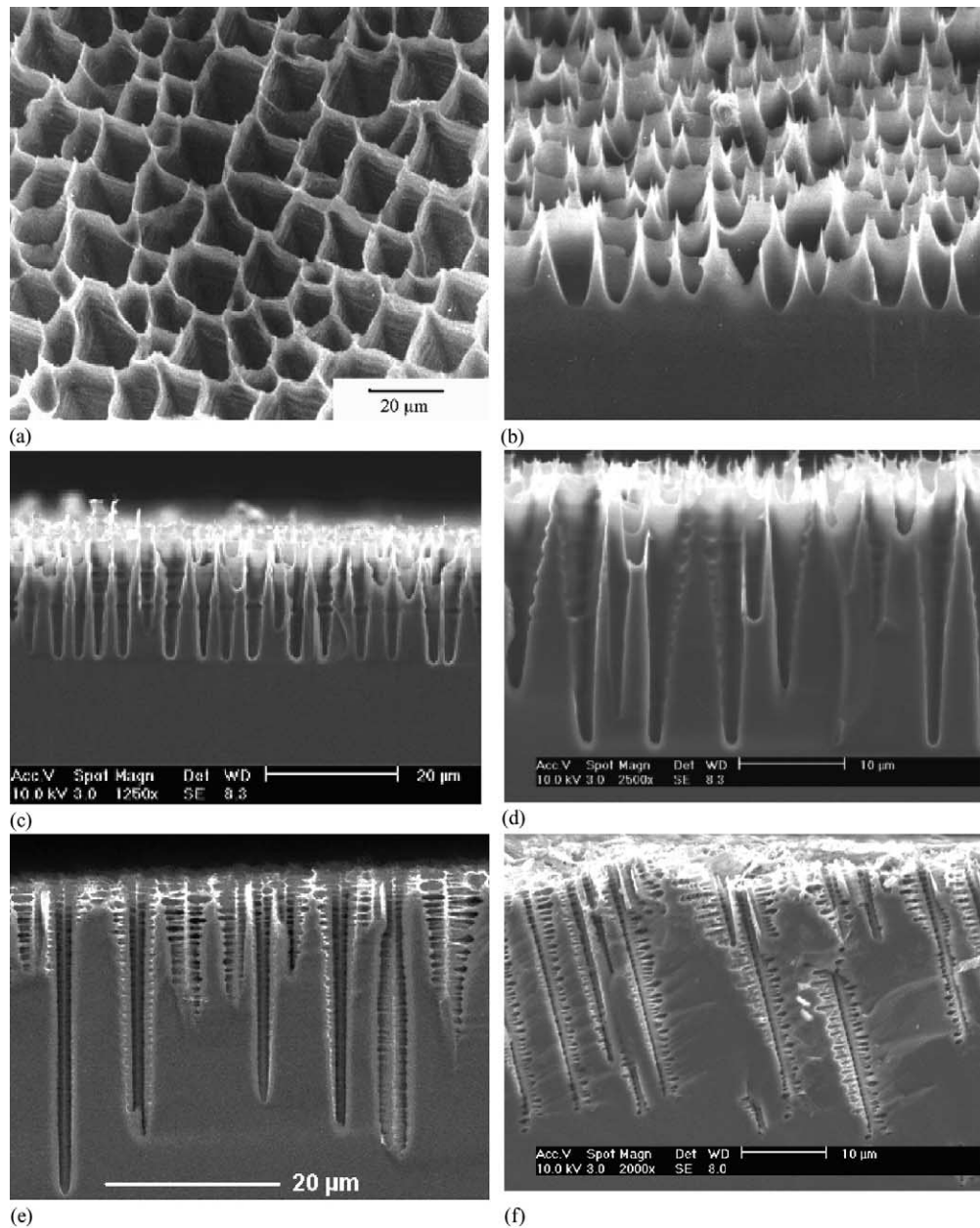


Fig. 13. Various n-macropores(fsi): (a) “old” picture from 1985 showing the surface of n-type Si etched in an aqu electrolyte and with front side illumination; (b) cross-section to (a). (c and d) n-macropores(aqu/fsi); (e and f) n-macropores(org/fsi/DMF) on  $\{1\ 0\ 0\}$  or  $\{1\ 1\ 5\}$ , respectively. For (c)–(f), 3–6  $\Omega\text{ cm}$  samples, 5 mA/cm<sup>2</sup>, 4 V.

568 electrochemistry of Si, and second, they were found in a systematic experiment on the base of  
 569 another prediction, this time coming from the CBM.

570 Until their discovery, it was generally believed that pores in heavily doped Si (of both doping  
 571 types) would always be mesopores. There was no theoretical justification for this, simply because  
 572 non of the existing models (with the exception of the avalanche break-through model introduced in  
 573 2000 [61]) said anything to n<sup>+</sup>-, p<sup>+</sup>-pores at all. However, there was much experimental evidence:  
 574 whatever you tried—mesopores were the result.

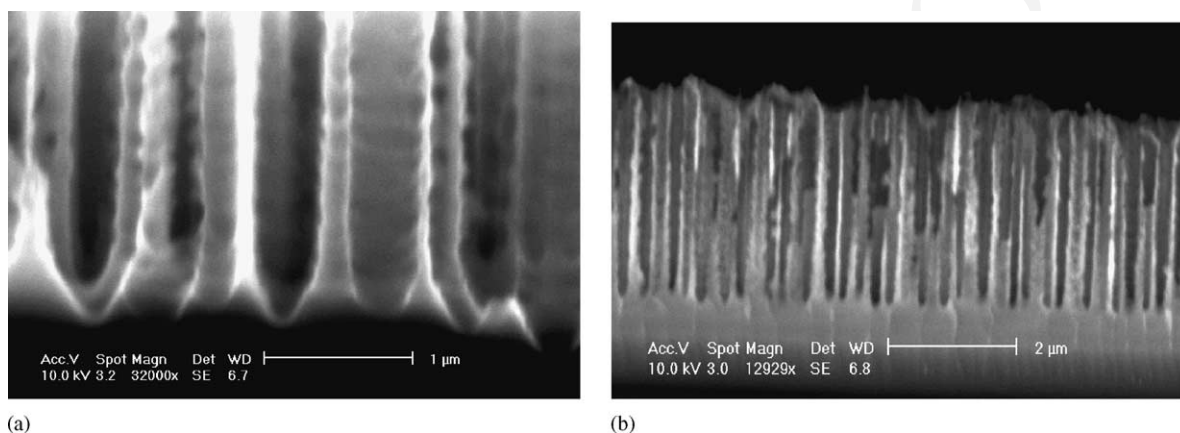


Fig. 14. Macropores in highly doped Si (0.020–0.060 W cm): (a) TMAH addition; (b) CrO<sub>3</sub> addition.

575 The CBM considers mesopores to dominate whenever the formation of SiO<sub>2</sub>, i.e. oxidation—is  
 576 weak as compared to direct dissolution. Oxidation, in turn, is weak if the supply of holes is small  
 577 compared to what the electrolyte can “process” by direct dissolution. Since the maximum direct  
 578 dissolution current is exponentially increasing with the potential at the Si surface, this condition is  
 579 always met for heavily doped Si. In this case, the voltage drop across the (very small) SCR is  
 580 negligible and almost all of the applied potential is available at the Si surface, allowing much larger  
 581 direct dissolution currents as even p<sup>+</sup> Si can deliver.

582 This leads to the expectation that strengthening of the oxidation by adding strongly oxidizing  
 583 chemicals to the aqueous electrolyte could supply sufficient oxidation which then would induce  
 584 macropores.

585 Indeed, n<sup>+</sup>-macropores(aqu + ox) could be achieved with several oxidizing ingredients; Fig. 14  
 586 shows examples. The most useful oxidizers were CrO<sub>3</sub> and TMAH, more details can be found in  
 587 [34]. However, no p<sup>+</sup>-macropores(aqu + ox) could be produced with electrolytes that worked for the  
 588 n<sup>+</sup>-case.

589 While applications are not considered at this point, n<sup>+</sup>-macropores(aqu + ox) demonstrate not  
 590 only that electrolytes can be “designed” with some guidance, but Fig. 14b gives a hint that this  
 591 results might be useful in producing macropores at very small pitch values.

### 592 2.7. Macropores in n-silicon obtained with organic electrolytes and back side illumination

593 This case, first reported in 2000 [22] produced very unexpected results which, in the view of the  
 594 authors, might prove to be of considerable importance for the general understanding of the  
 595 electrochemistry of Si and its possible technical uses. Using an electrolyte that produced rather  
 596 perfect p-macropores(org), its application to n-type Si with back side illumination resulted in pores  
 597 with several new features, cf. Fig. 15.

598 The few experiments performed so far with n-macropores(org/bsi) yielded a wealth of new data.  
 599 The general observations were as follows.

- The pores are wildly branched (in  $\langle 113 \rangle$  directions) and frequently issuing forth from two-  
 601 dimensional cavities bounded by  $\{111\}$  planes on one side (called “wings” in [34]; cf. Fig. 15b).
- Besides n-macropores(org/bsi) and “wings”, mesopores were often present at the same time (see  
 603 Section 4).



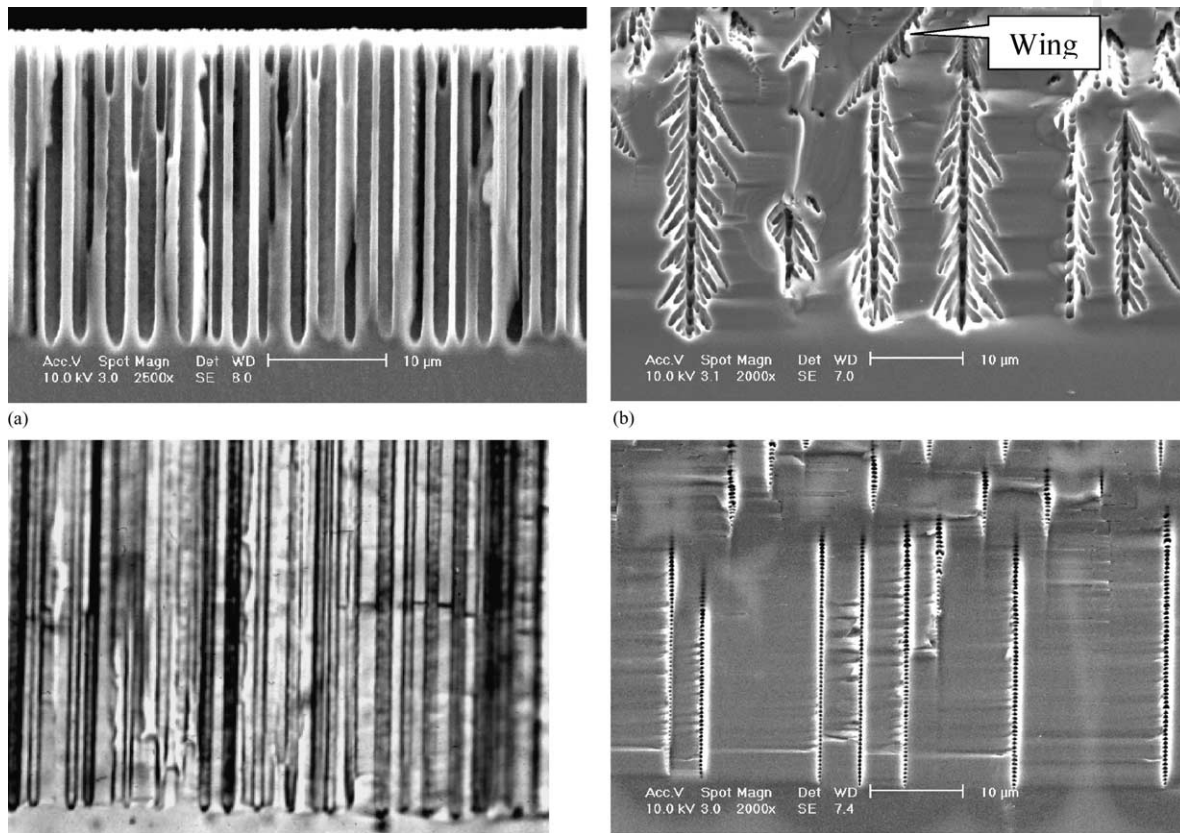


Fig. 15. Comparison of p-macropores(org) and n-macropores(org/bsi) for similar etching conditions ( $10\text{--}20\ \Omega\ \text{cm}$  samples,  $j = 2\ \text{mA}/\text{cm}^2$ ,  $U = 2\ \text{V}$ ): (a) p-macropores(org); (b) n-macropores(org/bsi) without superimposed ac current; (c and d) as (a) and (b) but with an ac current (33 mHz, amplitude =  $0.2\ j$ ) superimposed on the etching current  $j$ .

- The n-macropores(org/bsi) respond in an extremely non-linear fashion to ac currents superimposed on the etching current: whereas for frequencies below 33 mHz no visible changes occur, at 33 mHz the n-macropores(org/bsi) assume a regular shape without side pores and contain diameter modulations corresponding to the current modulation (Fig. 15d). This can only be described as a kind of chaotic resonance. The same current modulation with p-macropores(org) produced no noticeable effect (Fig. 15c).

Only few data about n-macropores(org/bsi) are available at present and no pore formation model besides the CBM has attempted an explanation so far. Of course, just considering the morphology, the SCR-model would have expected that perfect pores should result, given the additional stabilizing influence of the SCR and carrier focussing in a system that already produced rather perfect p-macropores(org). The observed resonant behavior at present seems to be beyond the reach of the “static” models (all except the CBM).

The resonant behavior of n-macropores(org/bsi) offers a new variable for controlling the growth of all pores in Si that has not been considered so far: modulations of the current, the voltage, or the light intensity with the right frequency and amplitude, may stabilize pores that would be unstable otherwise. While this new feature might be useful for applications, a much better understanding of the dynamics of pore growth is necessary for its employment.



### 622 3. Applications of macropores

#### 623 3.1. General remarks

624 Macropores offer a number of attractive features for many kinds of applications. A listing  
625 includes:

- extremely large aspect ratios (length/diameter) of  $>600$  for diameters in the  $1\ \mu\text{m}$  region;
- defined geometries (arrays) are possible—periodic, periodic with defects, or aperiodic—the only  
628 limitation being that the average pore density should be constant;
- large porosities and thus large volume to surface ratios are possible;
- large areas can be homogeneously etched due to the supreme homogeneity of Si wafers;
- full compatibility with Si technology.

632 There are, however, also some difficulties in employing macropores for products. These may be  
633 listed as follows.

- Si technology is often needed, i.e. a cleanroom with some standard processes like lithography,  
635 oxidation,  $\text{Si}_3\text{N}_4$  deposition—in other words an expensive infrastructure for research and  
636 development.
- Etching macropores on large areas (e.g. on a 200 mm wafer), while certainly possible, is neither  
638 easy nor (initially) cheap.
- While “perfect” n-macropores(aqu/bsi) are possible, they occupy only a tiny area in the total  
640 parameter space as outlined in Section 2. Abandoning this area in search of features not attainable  
641 there, will quickly incur a “black art” component, not easily accepted for product development.

642 Applications are now emerging in many areas, where three qualitatively different fields might  
643 be distinguished: microelectronic and mechanical systems (MEMS), optics, and “surface”; with  
644 “surface” meaning the use of large surface to volume ratios without much additional patterning for  
645 various projects. There is some overlap and we include all applications in the MEMS category that  
646 need some kind of structuring beyond just using porosity.

648 So far, almost exclusively n-macropores(aqu/bsi) were used and in what follows this type is  
649 meant whenever simply mentioning “macropores”.

#### 650 3.2. Applications to MEMS

651 One of the earliest applications of macroporous Si was pioneered by Ottow et al. [62,63] who  
652 used densely spaced regular macropore arrays as a kind of substrate into which deep three-  
653 dimensional structures on a larger scale were made. While this “Ottow”-process is not without some  
654 sophistication, in essence the raised areas were covered with a lithographically structured mask and  
655 the highly porous Si in the unmasked areas was etched off. Fig. 16 shows early structures obtained in  
656 this way; meanwhile the process has been perfected and is routinely employed for photonic crystals  
657 (see later and Fig. 19).

658 A particular innovative use of macropores is in the area of “Brownian motors or pumps” [48].  
659 Essentially, involved thermodynamics show that Brownian motion *plus* some asymmetric field can  
660 achieve what Maxwells demon cannot: sorting particles according to type or size [64]. In the variant  
661 using macropores pursued by the Halle group [65], a membrane containing macropores with a saw-  
662 tooth like cross-section separates two reservoirs with particles of two different sizes suspended in  
663 some liquid. Pulsing the pressure should pump one kind of particles to the left and the other kind to  
664 the right. As mentioned before, obtaining the controlled diameter variations of the macropores was

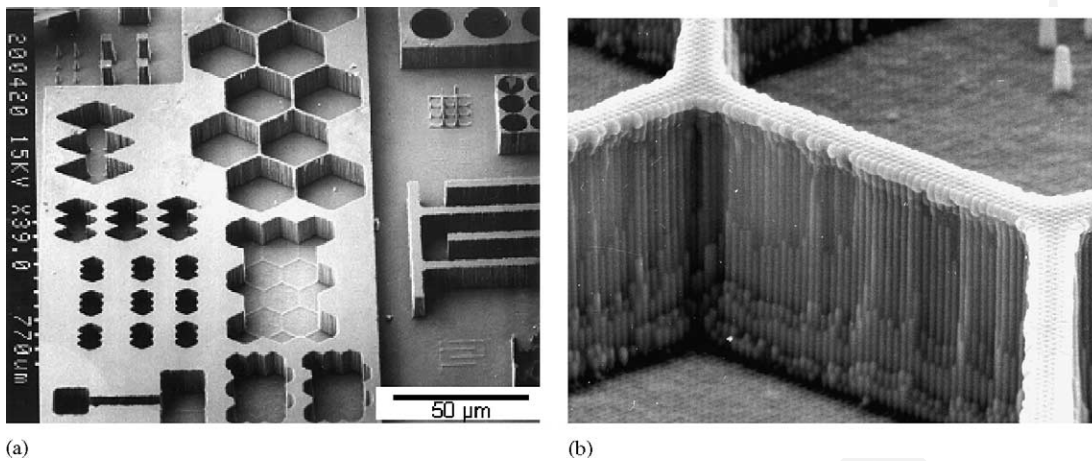


Fig. 16. Structures with large aspect ratios obtained by the “Ottow technique” [62,63] from macroporous substrates (early development stage): (a) overview, (b) detail from the hexagonal array.

665 not as easy as could be expected in most formation models, but Müller et al. [48] did finally succeed  
 666 in producing suitable membranes and are currently trying to demonstrate Brownian pumping. An  
 667 example (with a comparison to pores in GaAs) is shown in Fig. 17.

668 In this application like in many other, it is necessary to have pores that completely traverse the  
 669 Si substrate; something that cannot be achieved by etching alone. The n-macropore(aqu/bsi) growth  
 670 will always stop if the pore tip approaches the sample backside. This is understandable because holes  
 671 can no longer diffuse to the pore tip if the space charge region occupies the total volume of Si  
 672 between the pore tip and the sample backside. While for all other kinds of macropores this limitation  
 673 has not been experimentally demonstrated, it must be expected to occur as well. In any case,  
 674 macropores that would “grow out” on the backside are not desirable because of subsequent

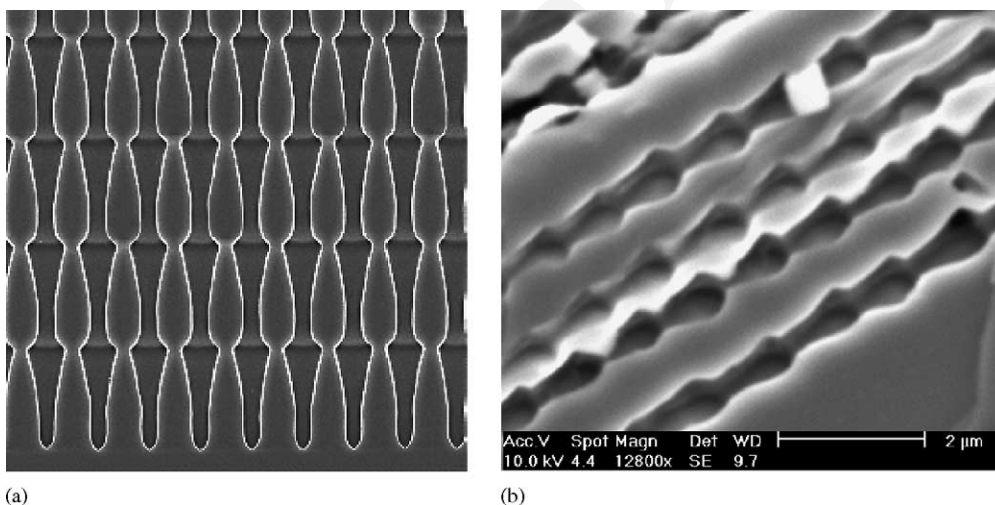


Fig. 17. (a) Macropores in Si with intentionally modulated pore cross-section intending a saw tooth shape (the distance between the center of the pores is  $4.2\ \mu\text{m}$ ; courtesy of Müller et al. [45]). (b) Macropores in GaAs without intentional diameter modulation. A saw-tooth shape evolves naturally demonstrating the close link between pores and oscillations (from [96]).

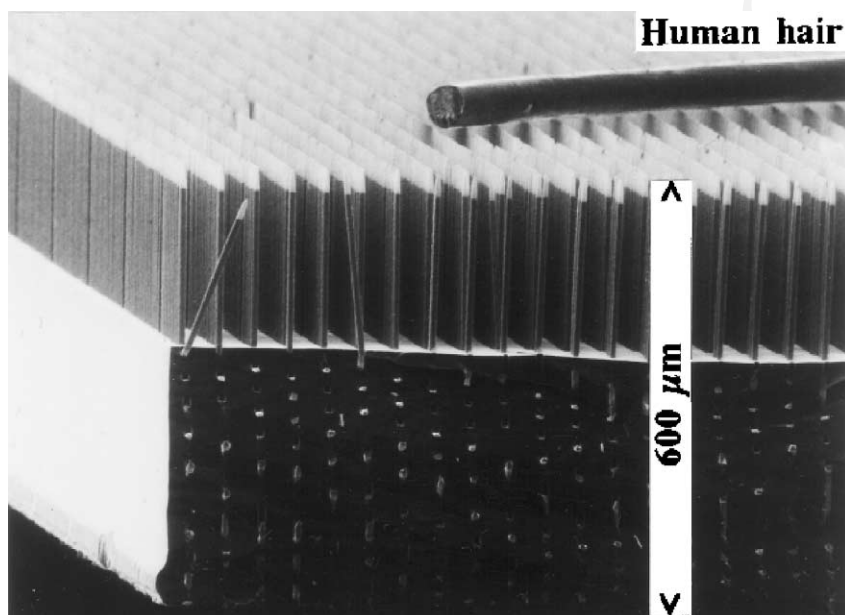


Fig. 18. Macropore array filled with lead taken from [66]. In the upper half of the sample, the Si was removed and the lead wires are exposed.

675 electrolyte leakage (or, in the case of electrolytic double cells, short circuits between the back- and  
676 frontside). It is therefore necessary to remove parts of the backside by mechanical polishing or  
677 plasma etching; a delicate operation for highly porous samples.

678 A novel use for macropores are X-ray filters. In medical X-ray imaging, all inelastically  
679 scattered photons reaching the film blur the image. (Consider a simple analogy: a strong light source  
680 will transmit some light through your hand. Without the inelastically scattered light, i.e. looking only  
681 at the directly transmitted light, you could see the bones.) A filter highly transparent to X-rays  
682 propagating along the optical axis, but not transparent in all other directions, could considerably  
683 increase the contrast of weakly scattering objects (encountered, e.g. in mammography). Recent work  
684 by Lehmann and Rönnebeck [66] used macropores filled with lead to produce such a filter. In this  
685 case, it may be necessary to use an aperiodic pore array with constant pore density to avoid Moirée  
686 effects with the periodic diode array in the CCD cameras universally used in X-ray devices. Fig. 18  
687 shows an example of the structures achieved. If fully optimized, the filter could reduce the X-ray  
688 dose by a factor of three without loss of resolution, or allow better images, respectively.

689 Macropores are also envisioned to be useful for chemical microreactors. At least one group [67]  
690 is working on this subject and at least one patent application is on record [68]. The large surface of  
691 porous silicon offers unique possibilities to synthesize specific chemicals in a microformat at chip  
692 dimensions. The reactions would be catalyzed by enzymes coating the pores; this is generally  
693 possible as demonstrated in [67]. Bengtsson et al. made a particular interesting approach to this topic  
694 by etching macropores in the wall of trenches pre-fabricated on {1 1 0} silicon. The trenches direct  
695 the flow of the reacting species; they were etched anisotropically with alkaline solutions and  
696 therefore have rectangular cross-sections. The macropores are coated with (immobilized) enzymes  
697 and the reaction rate is greatly enhanced by the increased active surface area. Highly efficient  
698 biocatalytic microreactors are obtained if the macroporous matrix is optimized with respect to pore  
699 geometry, morphology, and depth.

700 A relatively new issue for macropore applications is biotechnology [69]. Looking at regular  
701 macropore arrays, it is suggestive to use them for “biochips”. A biochip, loosely speaking, is a  
702 matrix of tiny test tubes in a regular array each of which is coated with a biochemical that reacts only  
703 with specific molecules or DNA sequences. Absence or presence of a reaction can be monitored  
704 optically (e.g. by luminescence or IR absorption) or electronically, and the position in the matrix  
705 identifies the chemicals present in the solution to be analyzed. This allows for quick and fully  
706 automated detection of thousands of molecules simultaneously. Besides suitable pore arrays,  
707 technologies for the coating of the pore walls and some suitable detection scheme must be  
708 developed; efforts in this direction are under way. Work in the Infineon laboratories has progressed  
709 to a point where first prototypes have been made and the technique may see product applications in  
710 the near future [69].

711 Sensors based on optimized macropore arrays have been under development for some time. In  
712 particular, Angelucci et al. [70] developed a sub-ppm benzene sensor for air quality monitoring. The  
713 key part of the device is a permeable macroporous silicon membrane, a few tens of microns thick,  
714 and with the pore walls coated by a semiconducting SnO<sub>2</sub> film. This film changes its resistivity in the  
715 presence of benzene (and other gases) and the large surface together with the optimized gas flow  
716 pattern through the pores allows extreme sensitivities. As stated before, a special process step is  
717 needed to open the pores at the back end of the specimen.

718 Kleinmann et al. [47] developed arrays of scintillating guides for digital X-ray imaging systems.  
719 Such scintillating guides have to be compatible with a special CCD cell spacing. Scintillating guides  
720 were etched electrochemically in n-type silicon. The pores were filled subsequently with a  
721 scintillating material.

722 Astrova et al. [71] studied the diffusion of boron and impurities into the walls of macroporous  
723 silicon with applications for power devices in mind. However, little has been published, to this issue  
724 although there is an old patent [72]. Of course, the general structure of the X-ray filter shown in  
725 Fig. 18 could also be used for a novel power device: the metal fingers, separated from the Si by a thin  
726 dielectric layer, could be used as gates, surrounding each finger with a depletion zone of variable  
727 depth. Current flow perpendicular to the filled pores then could be modulated by the voltage on the  
728 metal fingers akin to the grid voltage of an electron tube modulating current flow from the cathode to  
729 the anode.

730 So far, it has been very difficult if not impossible to produce macropores in structured areas  
731 without underetching the mask. However, recently Starkov et al. [73] showed that a particular  
732 combination of photoresists and etching conditions produced macropores with a depth of up to  
733 100 μm without any underetching of the mask.

734 Finally, first possible uses for the trenches (Fig. 6) are emerging. Xie et al. are working on the  
735 integration of analog and CMOS devices in one chip which calls for dielectric insulation and  
736 complete metal encapsulation of the analog part of the chip. While the first task could be performed  
737 by utilizing microporous Si, the latter task is more difficult to tackle. Etching a trench around the  
738 analog portion which is subsequently filled with metal may be an attractive candidate for this task;  
739 the technique is presently evaluated.

### 740 3.3. Large surface to volume ratios

741 Lehmann et al. developed a capacitor based on macroporous silicon. Essentially, macropores (or  
742 mesopores) are etched into a Si substrate and coated with a standard high-quality dielectric, usually a  
743 few nm thick ONO (oxide–nitride–oxide) layer. Deposition of (highly doped) poly-Si provides the  
744 second electrode. Specific capacities of 4 μF V/cm<sup>3</sup> are possible, comparable to Ta<sub>2</sub>O<sub>3</sub> capacitors,



745 and all other properties, especially the resonance frequency, are better than all competitors. The  
746 porous Si capacitors are naturally fully compatible with Si technology and, due to their extremely  
747 good dielectric, of very high quality.

748 The process has been developed to a production level, but the product has not yet been  
749 scheduled for mass production.

750 It has been realized rather early that macroporous layers with relatively shallow pores and  
751 preferably with diameters that are large at the surface and decrease with depth are ideally suited  
752 as anti-reflection layers for solar cells or for “black-body” emitters with optimized IR radiation  
753 [74]; such layers could be made most easily with-macropores(aqu/fsi), Fig. 13b) shows an  
754 example. However, since macropores in p-type Si were discovered much later and n-type Si is  
755 not used for solar cells, not much came of it. Note in this context that the use of microporous  
756 (or mesoporous) Si as an antireflection coating predates the discovery of its essential properties  
757 [75].

758 More recently, Levy-Clement and coworkers extensively studied the use of p-macropores(org)  
759 as antireflection layers on multicrystalline solar cell substrate material [76,77]. While good results  
760 were obtained, the approach is somewhat hampered because of unfavorable pore geometries for  
761 grain orientation around  $\{1\ 1\ 1\}$ . For the use of microporous Si as antireflection layer see Section  
762 5.2.

763 Macroporous layers etched from the backside into defined areas on a Si substrate may also be  
764 used either as a “low  $k$ ” material, i.e. as regions with strongly reduced dielectric constant (DK), or as  
765 “low  $\sigma$ ” area, i.e. with large transverse resistance. This can and has been used, e.g. for (relatively  
766 large) integrated inductors (spiral coils) which would suffer eddy current losses increasing with the  
767 square of the frequency if used on bulk Si.

768 Macroporous arrays in Si could also be used as a template for the production of “metallic  
769 barcodes as described in [78]. In this case, a succession of different metals is used to fill pores; after  
770 dissolution of the template (which was porous  $\text{Al}_2\text{O}_3$  in [25]), submicrometer metal rods with  
771 optically identifiable “stripes” are obtained which have many uses as a kind of label in, e.g.  
772 biotechnology.

### 773 3.4. Macropores and optics

774 The most prominent and unique application of macropores is in the area of photonic band-gap  
775 (PBG) materials, so-called photonic crystals [79,80]. In essence, photonic crystals consist of periodic  
776 variations of the index of refraction on a scale matched to the wave length of light, i.e. in the sub- $\mu\text{m}$   
777 region. In a loose but rather fetching analogy, a photonic crystal does to light waves what a real  
778 crystal does to electron waves. In particular, an optical band-gap may develop, not allowing the  
779 propagation of light in the relevant energy region, and states in the band-gap may be introduced by  
780 defects in the photonic crystal, that allow “processing” of light similar in some (but not all) respects  
781 to semiconductors. Photons, e.g. may only propagate along one or two dimensional defects, or may  
782 even become localized at zero order defects. While photonic crystals offer exciting research fields  
783 and a host of new applications, they are not easy to make.

784 The best two-dimensional photonic crystals are actually obtained by optimized macropore  
785 lattices, as first realized by Grüning et al. [81]. A complete optical band-gap was observed in all  
786 directions perpendicular to the pores. Since then, complex photonic crystals, including “macro”-  
787 structuring by the “Ottow” technique explained above and controlled defects, have been made by  
788 Birner et al. [82], Fig. 19 shows an example. Unfortunately, it proved exceedingly difficult to reduce  
789 the lattice parameter to dimensions below about  $0.8\ \mu\text{m}$ . The Halle group meanwhile succeeded in



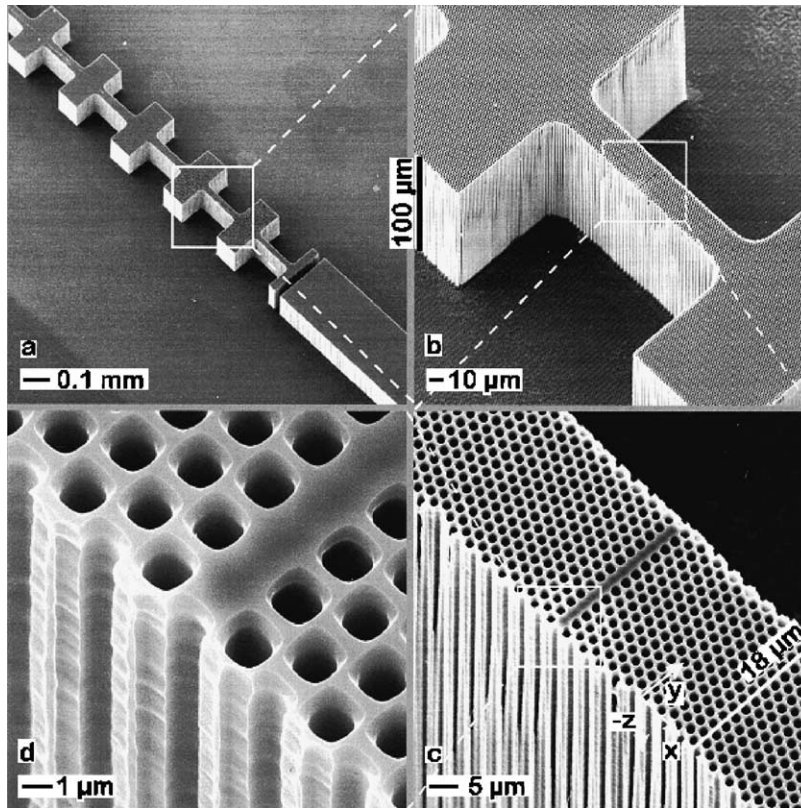


Fig. 19. (a–d) Two-dimensional photonic macropore crystal with a line defect (from [78]).

790 this task, but only by using a highly doped Si crystal especially grown by a float-zone technique  
 791 [83].

792 While macropore lattices are perfect for two-dimensional photonic crystals, three dimensional  
 793 pore crystals are harder to produce. One option is the exploitation of the peculiar  $\langle 113 \rangle$  growth  
 794 direction. Under favorable conditions macropores grow in all three symmetrically equivalent  $\langle 113 \rangle$   
 795 directions if seeded on  $\{111\}$  samples. If the nucleation is induced in a properly aligned hexagonal  
 796 lattice, three pores will meet at one point which then acts as nucleus for a new three-fold; a three  
 797 dimensional pore crystal with an orthorhombic symmetry (preferred for photonic crystals) results.  
 798 The results of a first experiment along this line is shown in Fig. 20.

799 There are, however, more ways to produce three-dimensional photonic crystal structures by pore  
 800 etching. In particular, a macropore lattice in microporous Si with a defined porosity modulation, or  
 801 defined diameter modulations of the macropores in a photonic crystal, may introduce the third  
 802 dimension in a way sufficient for some applications.

803 Macropore arrays have also interesting optical properties in the pore direction. Very roughly  
 804 speaking, photons with wave lengths smaller than the pore diameter pass through, others are  
 805 blocked. While it is actually more complicated than that (total reflection and diffraction effects at  
 806 small apertures must be considered), the general behavior is that of a (very good) filter for short  
 807 wave lengths, completely blocking longer wave lengths, cf. Fig. 21. Lehmann et al. produced and  
 808 described such a filter based on n-macropores(aqu/bsi) [84]. In contrast to Bragg or glass filters the  
 809 light is not transmitted in the matter but in the medium inside the pores, i.e. in air (or possibly  
 810 vacuum), which is advantageous for many applications.

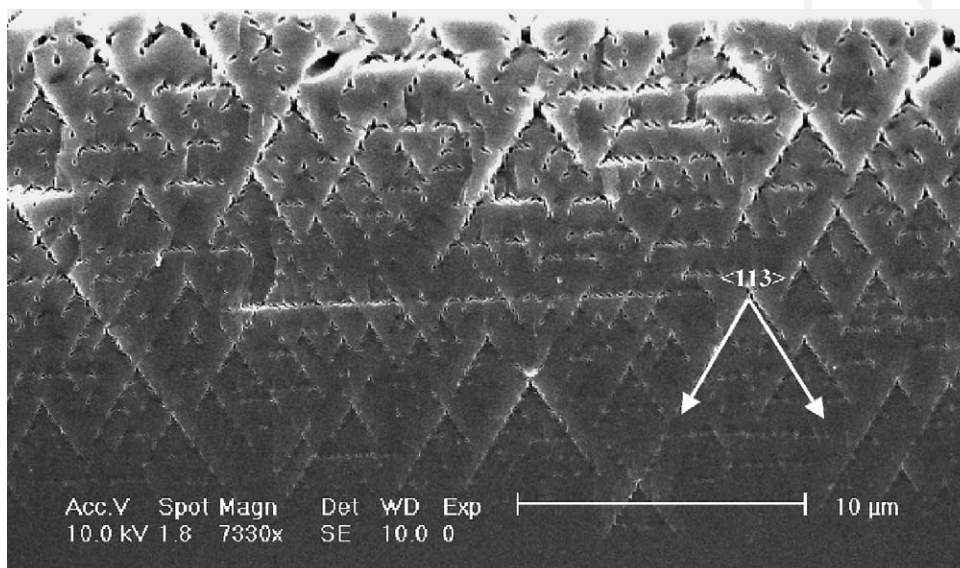


Fig. 20. First three-dimensional photonic crystal expressed in a intersecting  $\langle 113 \rangle$  oriented macropore lattice on  $\{111\}$ .

811 Finally, optical applications may profit from macropores in an indirect way, too, by using cheap  
 812 variants of the “Ottow” technique described above to produce moulds for casting microlenses.  
 813 Essentially, producing a deep circular depression would already be sufficient because a layer of glass  
 814 bonded to the Si mould would extent semispherically into the depression, driven and stabilized by  
 815 surface tension [85]. Using p-macropores(org) grown only in unmasked areas (with optimized  
 816 underetching) in connection with the trenches obtained under these conditions, may be the way to  
 817 success.

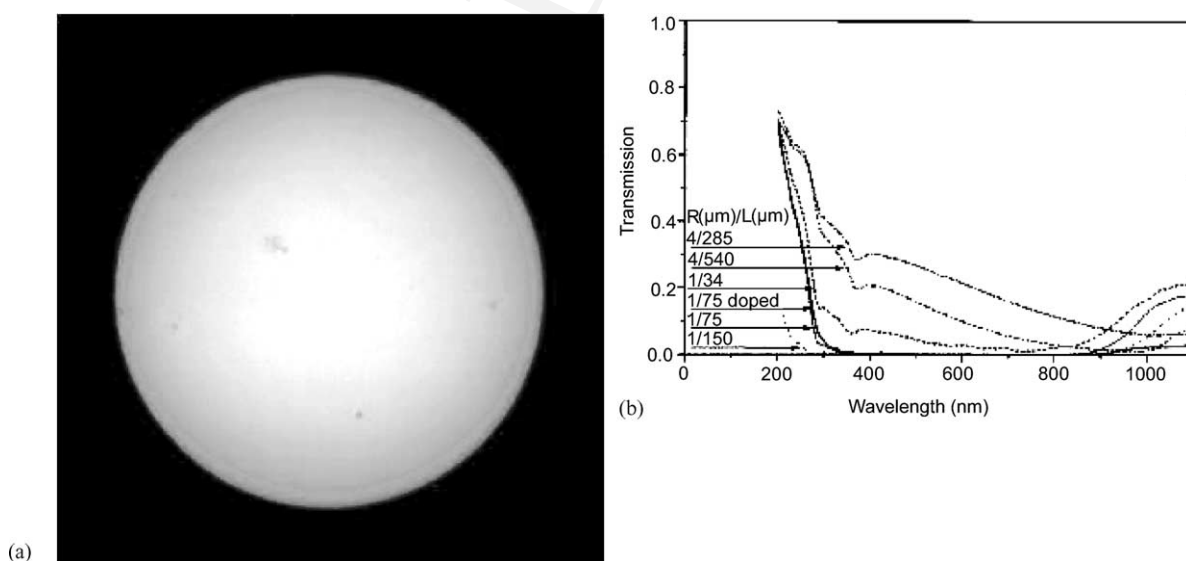


Fig. 21. (a) The sun viewed through a deep blue and UV transparent macropore filter. The original picture is deep blue; sunspots are clearly visible. (b) Transparency curves of various macropore UV transmitters.  $R$  and  $L$  denote the pore diameter and depth, respectively. Courtesy of V. Lehmann; cf. [79].

818 **4. Mesopores**819 *4.1. Formation and appearances*

820 By IUPAC definition, mesopores are all pores with  $10 \text{ nm} < d < 50 \text{ nm}$ , but, as stated before,  
821 this definition is too limited to be of much value. We will therefore use the following list as a  
822 working definition of mesopores; it coincides roughly with the geometric definition.

823 Mesopores are obtained for the following configurations.

- 824 1. Etching of highly doped Si in aqueous electrolytes always produces  $n^+/p^+$ -mesopores(aqu);  
825 Fig. 22a shows an example. No light is required in the case of  $n^+$  Si because avalanche break-  
826 through is easy and enough current will be produced even at small voltages. Lehmann et al.  
827 conducted a detailed study of these kinds of mesopores [61] to which the reader is referred.
- 828 2. Etching of moderately or low doped n-type Si in the dark produces “break down” (bd) pores (at  
829 voltages that might be as large as 100 V) which must not only be counted as mesopores by the  
830 geometric definition, but also within the frame work of the CBM. This kind of mesopores we  
831 denote n-mesopores(aqu/bd); Fig. 22b shows an example.
- 832 3. Etching of highly doped Si in organic electrolytes produces  $n^+/p^+$ -mesopores(org) which are  
833 quite similar to their  $n^+/p^+$ -mesopores(aqu) cousins [10,34], but may occur already at lower  
834 doping levels. While little work has been devoted to these pores, it appears that weakly oxidizing  
835 org electrolytes tend to encourage mesopore growth while strongly oxidizing electrolytes even  
836 allow macropore formation; Fig. 22c shows an example.
- 837 4. The n-mesopores(org/bsi) appear together with n-macropores(org/bsi); Fig. 22d shows examples.
- 838 5. Mesopores are found on occasion inside macropores, i.e. the macropores are filled with  
839 mesopores. This is actually just a special case of p-mesopores(org) obtained in weakly oxidizing  
840 electrolytes as discussed in Section 2.
- 841 6. Mesopores are on occasion observed to issue forth from macropores that stopped growing [86]; a  
842 particular tricky case for pore formation models; cf. Fig. 23a.

843  
844 As seen from the examples provided in Figs. 22 and 23 and from numerous published and  
845 unpublished sources, mesopores have some common characteristics (not without occasional  
846 exceptions, however).

- 848 • They only grow in  $\langle 100 \rangle$  directions [34] and since they are usually branched the branches are at  
849 right angles to the main pore. In instances where this seems to be not the case (e.g. Fig. 22c), the  
850 branches do not have a well defined geometric shape [61].
- 851 • Whenever mesopores assume some defined geometric shape (which seems to be tied to low  
852 current densities), it consists of connected octahedra as shown in Fig. 23b and c.
- 853 • At higher current densities the mesopores are still growing in  $\langle 100 \rangle$  directions, but the geometric  
854 shape of the branches is lost; they appear “cloudy” as illustrated in Fig. 22c

855 As in the case of macropores, some possible mesopore configurations are missing since they  
856 have not been investigated so far. This includes n-mesopores(org/bd), n-meso-pores(org/fsi), and—as  
857 a prediction of the CBM—n-mesopores(org/bsi) for weakly oxidizing organic electrolytes. Time will  
858 tell.

859 While there seems to be no conceptual problem with the formation of n-mesopores(aqu/bd)—  
860 after all, if avalanche break down is the only source of holes, the resulting pores must be small to  
861 allow high field strengths at the tips—the situation is not quite that clear: Why are n-mesopores(aqu/  
862 bd) always heavily branched (their counterparts in III–V semiconductors tend to be perfectly



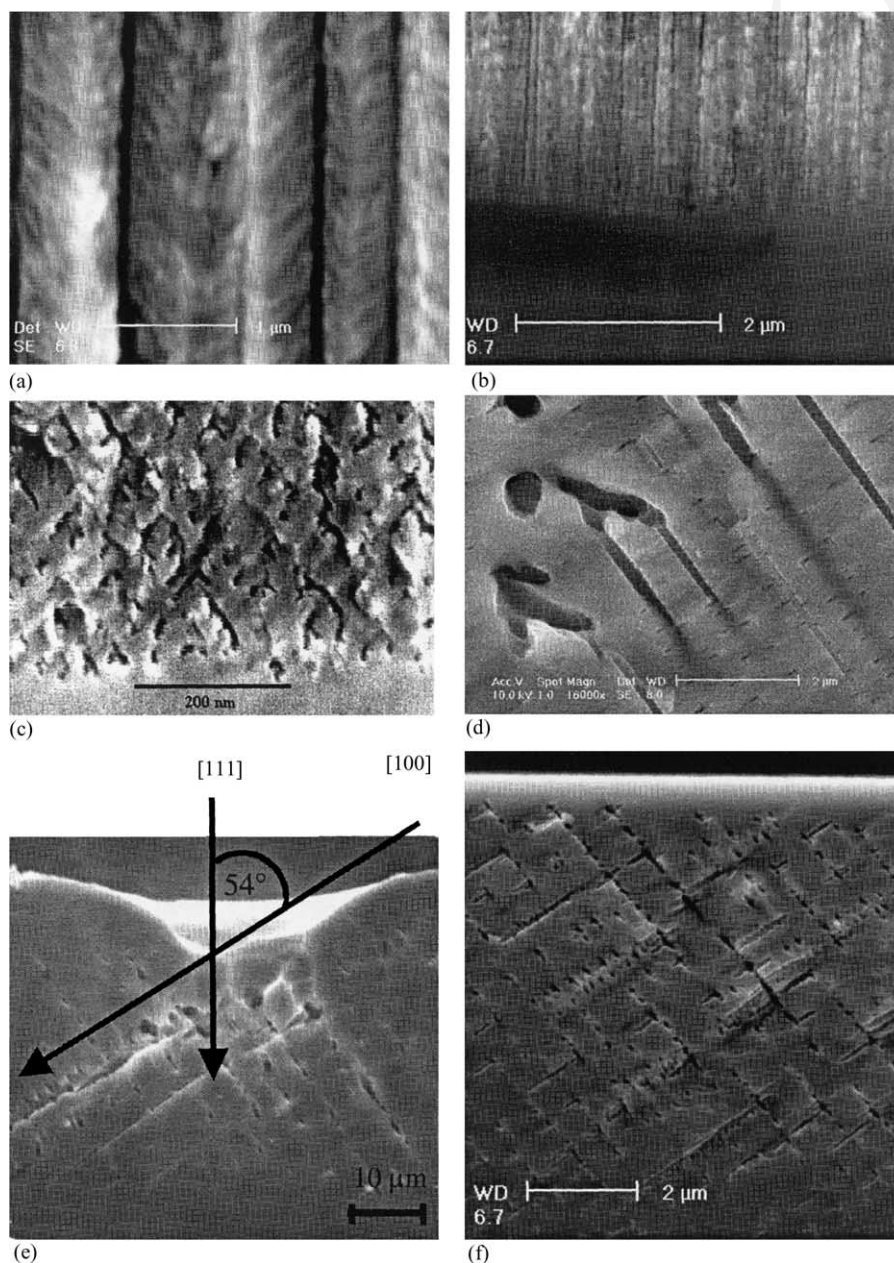


Fig. 22. Various kinds of mesopores: (a)  $n^+$ -mesopores(aqu/bt), low current densities ( $2 \text{ mA/cm}^2$ ); (b) p-mesopores(org/MeCN); (c)  $n^+$ -mesopores(aqu/bt) at high current densities ( $50 \text{ mA/cm}^2$ ), from [41] (courtesy of V. Lehmann); (d) n-macro(org/bsi),  $\{2\ 3\ 3\}$  substrate; (e) n-mesopores(aqu/bt),  $\{1\ 1\ 1\}$  substrate; (f) n-mesopores(org/DMF/bt);  $\{1\ 1\ 1\}$  substrate.

863 straight)? If the pores are close enough to each other (which they usually are), there should be no  
 864 sizeable electrical field between the pores and thus no inducement to branching. Moreover, there is  
 865 no good reason why n-mesopores(aqu/bd) exclusively produced by avalanche break down should not  
 866 always grow perpendicular to the sample surface, something they emphatically do not (again in  
 867 contrast to their III–V cousins) as shown in Fig. 22e and f.

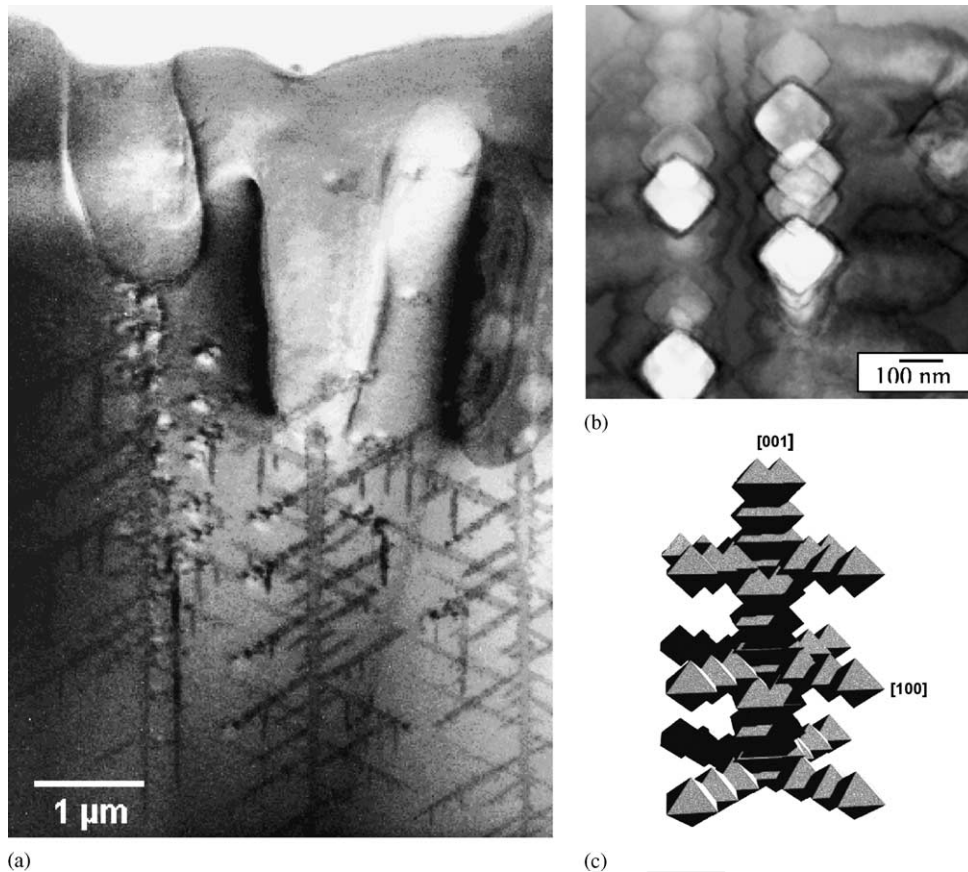


Fig. 23. (a and b) TEM micrographs of macropores with mesopores in n-type silicon (bsi, aqu) from [81]; (c) schematic view of a mesopore.

868 All things considered, there is no convincing model for the formation of mesopores at present,  
 869 although the CBM has some suggestions (see Section 7).

870 As far as the authors know, there has been no attempt to grow mesopores from pre-defined  
 871 nuclei. While this is simply due to the difficulties in obtaining lithography well below 0.1 μm for  
 872 dense arrays of mesopores, there is no particular reason not to try n-mesopores(bd) in some version  
 873 at larger spacings for any electrolyte.

#### 874 4.2. Applications of mesopores

875 The first large-scale commercial product based on pores in Si actually uses mesopores for  
 876 producing silicon on insulator (SOI) wafers. The ingenious Epitaxial layer TRANSfer (ELTRAN<sup>TM</sup>)  
 877 process from CANON<sup>TM</sup> [7] first produces a “normal” mesoporous layer of a few μm thickness,  
 878 followed by a layer with very large porosity by changing the current density in situ. After an H<sub>2</sub>-  
 879 anneal that closes the pores on the wafer surface, an epitaxial Si layer (which will be the functional  
 880 layer) is deposited. Next the wafer is bonded to an oxidized second wafer. A fine water jet splits the  
 881 wafer stack along the mesoporous layer with the large porosity—it is like opening a zipper. Finally,  
 882 a second anneal smoothes the surface obtained and the result is a SOI wafer with a very high quality Si  
 883 layer on thermal SiO<sub>2</sub>.



884 A similar process was investigated for solar cells by a Japanese company [7] and two German  
885 groups [87,88]. Again an epitaxial layer of about 25  $\mu\text{m}$  is grown on a highly porous layer which has  
886 been annealed to close the top porous layer. The solar cell is produced on the “thick” wafer and  
887 active solar cell structure together with the bulk silicon layer of 25  $\mu\text{m}$  is afterwards lifted off by  
888 breaking the highly porous structure. This technique allows to produce thin solar cells with  
889 efficiencies up to 15%.

890 Note that on occasion the mesoporous layers employed are referred to as “microporous”. While  
891 this is not necessarily wrong on the base of the formal 10 nm limit dividing micropores and  
892 mesopores, the ELTRAN<sup>TM</sup> process seems to employ mesopores—judging from the data given in  
893 [89].

894 This may also be the reason why mesopores are rarely mentioned in the context of applications  
895 but often treated under “micropores”. In general, it appears likely that mesoporous layers can be  
896 used in many cases where microporous layers “work”, too. Sensors, Bragg reflectors, waveguides,  
897 multilattices, biological applications and sacrificial layers have also been developed (possibly not  
898 always consciously) on mesoporous silicon, too [4,5]. In many cases where the lack of luminescence  
899 is not detrimental, mesoporous structures are to be preferred because they have a better mechanical  
900 stability in comparison to micropores.

## 901 5. Micropores

### 902 5.1. Some general remarks

903 Micropores and their possible applications have been covered in detail elsewhere [6–8] and this  
904 chapter will be brief accordingly. In particular, we will not cover the luminescent properties of  
905 microporous Si or applications that were envisioned and investigated (but never used in production)  
906 before the discovery of the luminescent properties of microporous Si, e.g. the “FIPOS” process  
907 (short for “full isolation by oxidized porous silicon”), cf. [90].

908 Generally, groups working with micropores use aqu electrolytes with large HF concentrations  
909 for two reasons: (1) microporous layers grow rather rapidly and uniformly and (2) their porosity is  
910 high (porosity tends to increase with the HF concentration and the etching current [36,49]). If the  
911 current and/or the HF concentration are too small, macropores(aqu) will result.

912 Both doping types of Si are being used, n-type Si may require some light or larger voltages, but  
913 no distinct difference in micropore properties have been reported. For heavily doped Si, mesopores  
914 will result under conditions that otherwise produce micropores. This necessitates that there is some  
915 transition from micropores(aqu) to mesopores(aqu) if the doping level is increased, and another  
916 transition from micropores(aqu) to macropores(aqu), if the current and/or the HF concentration are  
917 lowered. By inference, there must be a transition from mesopores(aqu) to macropores(aqu)—what  
918 would be needed is some kind of phase diagram as shown in Fig. 12, augmented by a third axis for  
919 the doping of the Si.

920 No model can explain micropore formation satisfactorily. While quantum wire effects seem to  
921 be necessary, they only could account for the distance between micropores (which must be so small  
922 as to produce quantum wire effects) but not for the diameters.

923 While until recently only p/n-micropores(aqu) have been observed, according to the CBM it  
924 should be possible to obtain p-micropores(org) too, if the organic electrolyte has sufficient oxidizing  
925 power. This is indeed the case, with a Formamide based org electrolyte (cf. Table 2) and  $j = 2 \text{ mA/cm}^2$ ,  
926 p-micropores(org/FA) were obtained for the first time. That the pores were indeed micropores

927 and not mesopores (which is hard to distinguish with a SEM alone), was shown by their strong  
928 luminescence in the yellow-orange and even blue regime (cf. Fig. 26d).

## 929 5.2. Applications of micropores

930 Following the discovery of the peculiar optical properties of microporous Si by Canham [1] and  
931 Lehmann and Gösele [2] in 1990, the application focus was on optoelectronic devices based on Si,  
932 and a large number of electro-luminescent (EL) devices has been presented, cf. [91]. Most of them  
933 consist of a microporous layer with a contact layer on top. Various materials have been used for  
934 contacts, e.g. thin metals like Au, indium tin oxide (ITO), silicon carbide and conducting polymers  
935 [92].

936 However, while working EL devices based on microporous Si have been demonstrated [91],  
937 stable and strong EL has not been achieved despite large-scale efforts. After  $\sim 10$  years of research  
938 the consensus seems to be that the stability of PL and EL is not a trivial problem. The most  
939 promising approach to overcome this problem might be the grafting of special molecules on to the  
940 microporous Si surface [93].

941 Bragg reflectors and Fabry–Perot filters have been realized by a modulation of the PS porosity.  
942 These applications are based on the variation of the optical properties with the porosity of the  
943 microporous (or mesoporous) films. The Jülich group first showed that multilayers with controlled  
944 variations of the porosity and microstructure can be obtained by varying the doping concentration, or  
945 by varying the etching parameters (mostly the current density) [94]. Superlattices can be formed in  
946 this way which may be used, e.g. as high-quality Bragg reflectors, Fabry–Perot filters, wave guides,  
947 or antireflection layers [8]. If microporous multilayers are grown on a substrate with a textured  
948 surface, a three-dimensional structure results with possible applications for photonic crystals [95].

949 Sensors based on microporous silicon use both the large surface to volume ratio of the  
950 microporous layer and the optical properties of this material. Since the Si surface is always covered  
951 by a thin oxide layer (after sufficient exposure to humid air) as-grown microporous Si is rather  
952 stable. The stability can be enhanced considerably, however, by a condensation reaction with alkoxy-  
953 or chlorosilanes to produce a new Si–O–Si [96].

954 If there is a reaction between the silicon and the gas to be detected, the process is generally  
955 irreversible. Sailor, e.g. used this for the detection of HF gas by monitoring in situ the dissolution of  
956 oxide in PS based interferometers as an irreversible process.

957 If there is no reaction, the process is reversible and it can be used for continuously monitoring  
958 gas concentration. Since the adsorption properties are different for different molecules, so is the  
959 charge state of the surface—adsorption induces specific changes in the resistivity (transduction mode  
960 of a sensor), of the photoluminescence, and of the reflectivity; all of which can be used for sensor  
961 purposes. In particular, the condensation of molecules inside the pores can lead to quenching of  
962 photoluminescence by energy or electron transfer. Even an “artificial nose” able to detect several  
963 gases simultaneously has been demonstrated [97].

964 Microporous Si is a splendid sacrificial layer and of potential value for MEMS fabrication. Free  
965 standing silicon structures, e.g. can be formed by anodizing and selective removal of the  
966 microporous silicon formed underneath a silicon membrane [98]. Presently, however, it appears that  
967 no product based on this application is available on the market.

968 It is of some historical interest to note that microporous Si was the key ingredient in the so-  
969 called “FIPOS” process mentioned above which used the selective formation of microporous Si  
970 (only  $n^+$  wells containing a p-region turned into microporous Si during anodization) and its far  
971 higher rate of oxidation to produce a p-type region fully embedded in oxide [90].

972 Canham reviewed porous silicon uses as an active biomaterial [99]. Essential properties are that  
973 highly porous silicon surfaces are compatible to and biodegradable in the human body. Living  
974 neurons have been cultured on microporous Si [100] and the tissue compatibility of PS has been  
975 demonstrated. Microporous Si as a biomaterial thus offers a new and dynamic field of research with  
976 important potential applications [101].

977 A new way of using microporous (and/or mesoporous) Si as antireflection coating for solar cells  
978 has been demonstrated by Striemer and Fauchet [102]. Essentially, the porosity is graded from very  
979 large at the surfaces to gradually from near 1 to the bulk value and reflection is efficiently  
980 suppressed.

981 A slightly exotic property of microporous Si may lead to special applications: it is highly  
982 explosive if kept under certain conditions [103,104]. First ideas for possible uses are expressed in the  
983 references given.

## 984 6. Experimental considerations

### 985 6.1. General

986 It is not uncommon that beginners in the field have initial problems to obtain homogeneous  
987 etching and reproducible results. Some factors that need attention are as follows.

- 989 • The back side contact of the sample may not be ohmic (“ohmic” meaning that the contact  
990 resistance shows a linear current voltage relationship and is small). Just putting Si on a metal plate  
991 is mostly not good enough, especially for low doped samples. Rubbing liquid In–Ga alloy on the  
992 back side, together with some scratching, usually will suffice. It is good practice to make two In–  
993 Ga spots and to measure the  $I(V)$  characteristics between the spots. If it is linear, at least one of the  
contacts is ohmic.
- 995 • While reference electrodes are not always needed, it is usually advisable to use one in order to  
996 obtain reproducible results and to be relatively independent of the (temperature dependent)  
997 electrolyte conductivity. While a standard calomel electrode (SCE) is the reference electrode of  
998 choice for detailed measurements and experiments, a Pt wire may be sufficient for many practical  
cases including applications.
- 1000 • A key issue is the addition of small amounts of surfactants to increase the “wetability” or to  
1001 decrease surface tension effects, respectively. Common surfactants (“dish water detergents”),  
1002 however, are not necessarily active in an acidic environment. The semiconductor industry  
1003 routinely uses surfactants in its HF bathes which are commercially available (e.g. by Merck) and  
1004 should be used. Exceptions are aqu electrolytes diluted with ethanol (which acts as wetting agent)  
and some org electrolytes for the same reason.
- 1006 • Electrolyte flow is crucial for many experiments; it should be homogeneous and steady. This is not  
1007 easily achieved with the commonly used peristaltic or membrane pumps. In some cases, the results  
1008 of etching experiments depend sensitively on the pumping speed which then becomes a parameter  
1009 to be controlled. A related problem are hydrogen bubbles which on occasion may cling to surface  
1010 of the sample producing inactive spots and noise in the controlled parameter (usually the voltage  
1011 or the light intensity). Bubbles must be avoided; pumping, surface reactants, and “sharp” seals at  
the edge of the sample help.
- 1013 • All electrolytes dissolve some  $O_2$  from the air which participates in the dissolution process. Since  
1014 the oxidizing power of an electrolyte is one of its crucial characteristics, displacing dissolved  $O_2$   
by bubbling of the electrolyte with  $N_2$  before use is often necessary for reproducible results.

- 1016 • For many applications, especially if very perfect and deep pores are to be etched, control of the  
1017 temperature is essential. Not only is it necessary to keep the temperature constant, room  
1018 temperature is not always the best choice. A heat exchanger system, allowing temperature control  
1019 between about 0 °C and 40 °C, should be part of an etching apparatus.
- 1020 • If illumination is used, three additional problems arise: homogeneous and controllable  
1021 illumination with a high intensity is needed, the backside contact must be at the edge of the  
1022 sample for back side illumination, and the electrolytic cell must have a light transparent window  
1023 for front side illumination.
- 1024 • All materials in contact with the electrolyte must be chemically inert in this environment. For  
1025 some electrolytes (especially, HF mixed with potent solvents like DMSO), this may limit the  
1026 choice of materials to Teflon and its derivatives. Transparent windows, heat exchangers, etc. then  
1027 are problematic and must be designed with care. Expensive sapphire windows and more Teflon  
1028 have to be used. It is often a good idea to test a cell at first with inexpensive PVC and less  
1029 aggressive electrolytes before the expensive final construction is made.
- 1030 • While the electrolyte is primarily chosen from pore etching considerations, it is advisable to pay  
1031 some attention to its conductivity and its pH value. The conductivity may be improved by adding  
1032 salts to the solution, e.g. NH<sub>4</sub>Cl to aqueous electrolytes with low HF concentration, or  
1033 tetrabutylammonium-perchlorate for MeCN, but for many organic electrolytes no suitable salts are  
1034 known. Conducting salts, of course, may influence the etching in unpredictable ways, too. The pH  
1035 value is mostly determined by the HF concentration, but it can be varied to some extent by the  
1036 addition of acetic acid or by other means. There is, however, neither a strong indication that the  
1037 pH value (for constant nominal HF concentration) is of prime importance for pore etching, nor  
1038 much systematic investigation into this topic [58,105].

## 1038 6.2. Large area etching

1039 Most applications envisioned call for the etching of standard size Si wafers, at least 100 mm,  
1040 better yet 150 or 200 mm. While any etching recipe that produces satisfying pores with small  
1041 samples of typically 1–4 cm<sup>2</sup> will of course also work for larger wafers if the proper conditions can  
1042 be maintained everywhere on the surface, there are a number of specific technical problems to large  
1043 area etching that are not easy to solve. Etching n-macropores(bsi) is the most demanding task  
1044 because of the necessary back side illumination. Problems encountered (and possible solutions) are  
1045 as follows.

- 1047 • The fraction  $j_{\text{etch}}$  of the hole current  $j_{\text{photo}}$  which is generated by illumination at the back side  
1048 ( $t = 0$ ) of a wafer with thickness  $d_w$  and a minority carrier diffusion length  $L$  that reaches the pore  
1049 tips at a depth  $l$  as measured from the wafer surface is proportional to

$$1051 \frac{j_{\text{photo}}}{j_{\text{etch}}} \propto \cosh\left(\frac{d_w - l}{L}\right) \approx \exp\left(\frac{d_w}{L}\right) \exp\left(-\frac{l}{L}\right). \quad (6.1)$$

1052 In order to achieve a uniform and large current density for etching, the wafer thus should have a  
1053 uniform and large diffusion length  $L$  and a “perfect” backside to minimize recombination losses  
1054 at the back side. This is not automatically guaranteed with commercial n-type wafers, especially  
1055 for larger doping concentrations.

- 1057 • The light source must provide a homogeneous and intense coverage of the back side and must be  
1058 controllable since for most applications the current is controlled by the light intensity. Arrays of  
1059 light emitting diodes proved to be the best choice.



- The back side contact is very critical. If back side illumination is employed, it either can be supplied by a contact ring around the perimeter of the wafer (e.g.  $n^+$  implantation and Al deposition through a mask followed by an anneal) which is expensive, by contact needles (necessarily damaging the Si) or by a (light transparent) electrolyte or ITO contact. While the Lehmann group favors contact needles, the group at Philips research uses an electrolyte contact [49]. Since a less aggressive electrolyte can be used for the contact, some of the problems encountered on the front side might be less severe for the backside contact in this case.
- While the current density is not very large (some  $10 \text{ mA/cm}^2$ ) the total current easily reaches 10 A. If contact problems exist, this may generate enough local heat to soften the polymers used for the cell, leading to leakage and serious safety problems.
- Besides removing the heat produced by ohmic losses, a constant temperature carefully adjusted to some optimum value (not necessarily around room temperature) is absolutely essential for successful etching and this requires large pumping and heat exchange equipment.
- The chemical reactions always release gases—mostly  $\text{H}_2$ —and for large wafers large amounts are produced which may lead to violent bubbling. An efficient means of safely removing the gases is necessary.
- Uniform pores will only result if the supply of reactants and the removal of products are homogeneous and stable. Circulation and/or movement of the electrolyte are mandatory and the flow pattern across the wafer must be either uniform in general, or uniform on time average.
- For making pre-structured n-macropores(aqu/bsi), usually an oxide mask is used. Pore etching commences at the openings of the mask and by the time the mask has dissolved the pores are deep enough for stable growth. Etching random pores, or pores through  $\text{Si}_3\text{N}_4$  masks, may require an optimized nucleation step before the conditions for stable pore growth are established.
- While polished surfaces are not always necessary, it is a good idea to thoroughly clean the wafers if homogeneous random nucleation is desired, cf. Fig. 24.

Macropores on p-type Si—either in aqu or org electrolytes—do not require illumination which makes cell design easier (but with the added complexity of sever restrictions in useable materials). A design suitable for 150 mm wafers is now operative (after a year of optimization) in the Kiel group. Fig. 25 shows a schematic drawing.

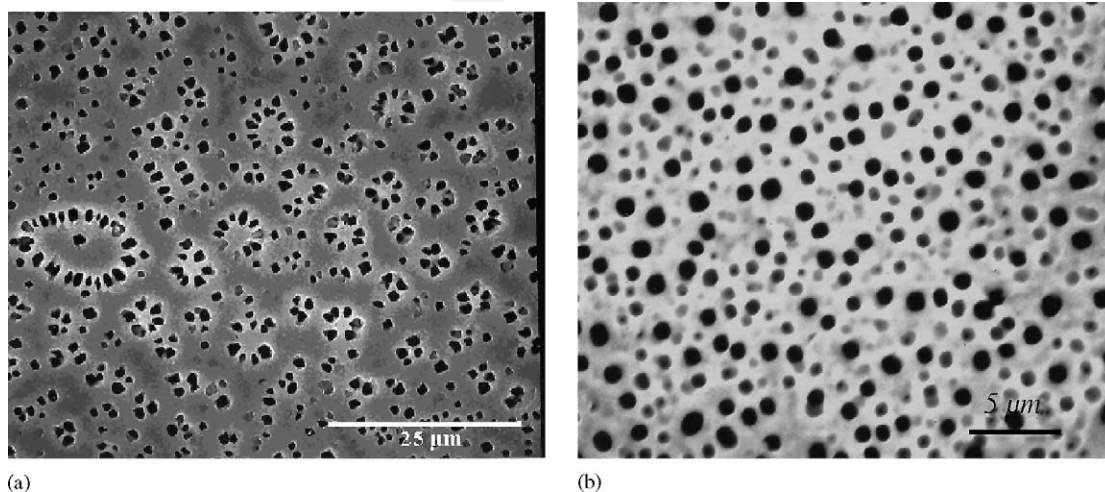


Fig. 24. Random n-macropore(aqu/bsi) nucleated on (a) uncleaned and (b) cleaned samples.

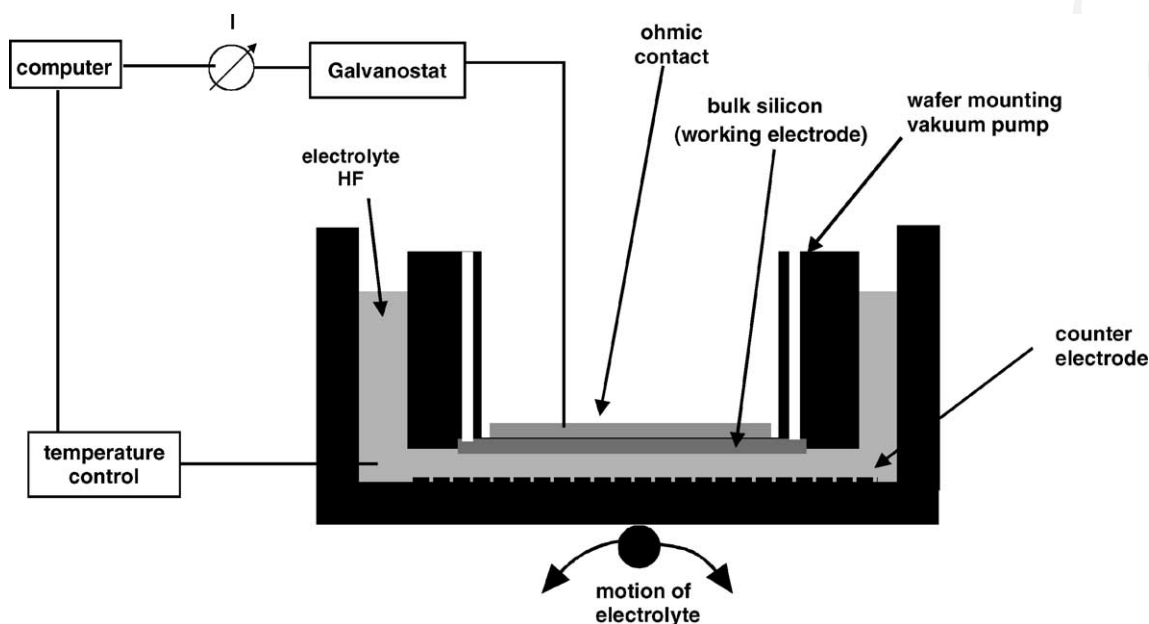


Fig. 25. Schematic drawing of the 150 mm cell developed for pore etching without illumination.

1089 The cell has been constructed from PVC for the trial and error period which presently limits the  
 1090 use of organic electrolytes. So far, mostly p-macropores(aqu) were etched (p-macropores(org)  
 1091 (Fig. 26) have to await a reconstruction with Teflon only for the crucial parts. Fig. 25 shows some  
 1092 results demonstrating the homogeneity achieved.

1093 Etching micro- and mesopores of just a few micrometers in depth on large areas is a  
 1094 comparatively easier task. Obviously the ELTRAN™ [7] process has mastered this; but little is  
 1095 known about the cell design except that an electrolyte backside contact is used and several wafers are  
 1096 processed at the same time.

## 1097 7. The current burst model

### 1098 7.1. General features of the current burst model

1099 A complete model of the electrochemistry of Si should not only be able to explain the  
 1100 bewildering multitudes of pores, but also the current or voltage oscillations and the peculiarities of  
 1101 the  $I(V)$  characteristics. It must, moreover, accommodate the many models applicable to pore growth  
 1102 in some way, because those models are not wrong—SCR regions do exist and will focus holes on  
 1103 pore tips, avalanche break-through will occur at high field strength, and diffusion instabilities are  
 1104 real, too, as any snowflake or dendritic crystal will testify. Such a model then cannot be simple.

1105 The current burst model (CBM) essentially claims to explain the electrochemistry of Si in the  
 1106 way defined above. It is an emerging model with many features not yet fully understood and some  
 1107 loose ends. Nevertheless, it explains current oscillations (at low frequencies) in a fully quantitative  
 1108 way [23,24], offers explanations in several issues of pore formation where all other models remain  
 1109 silent, and provides guidelines for the design of experiments and electrolytes (including III–V  
 1110 compounds) that have proved very useful in the investigations of the authors. In what follows we will

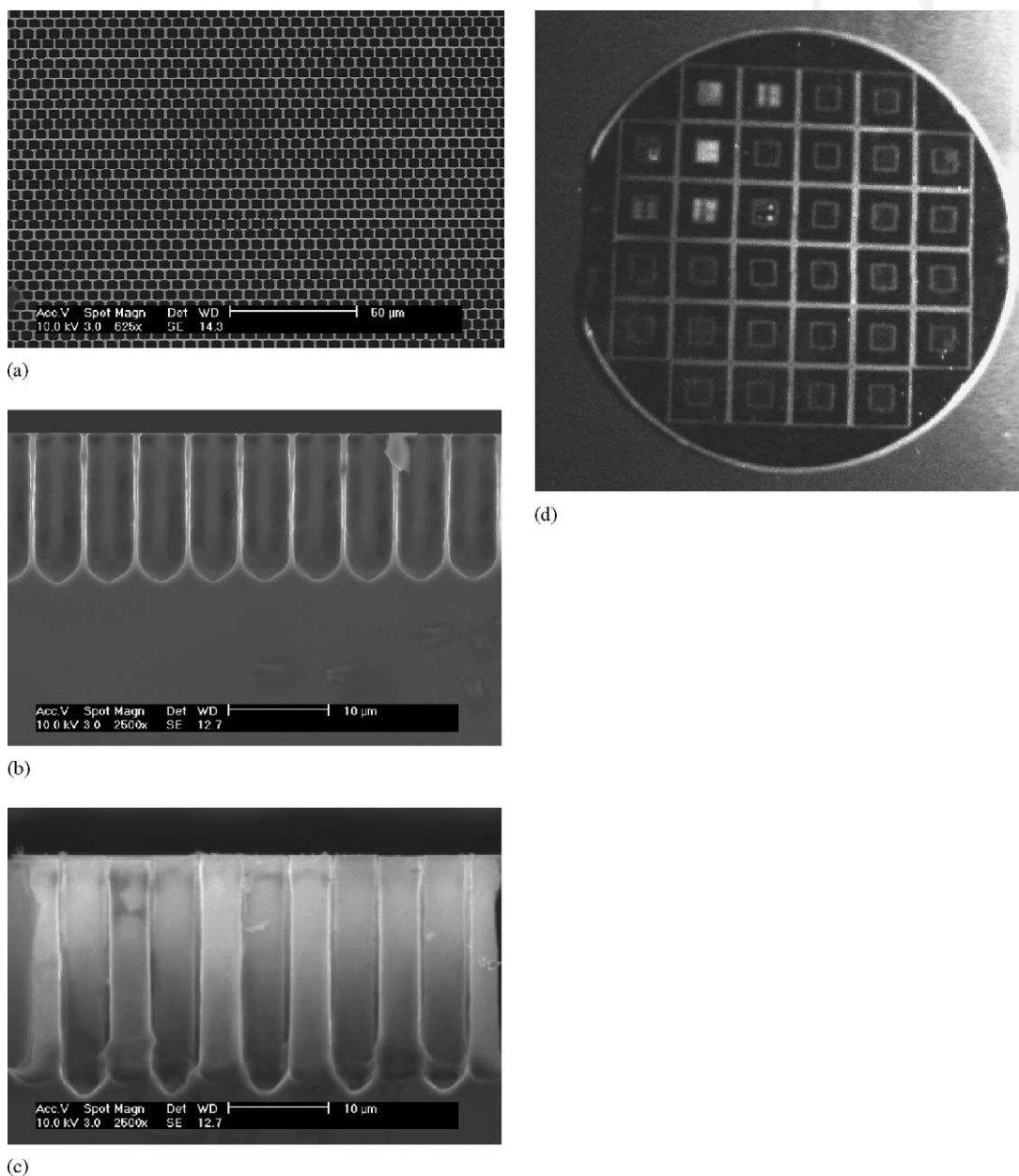


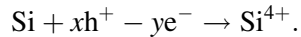
Fig. 26. The p-macropores(aqu) etched with the 150 mm cell from the center (a) plane view and two corners (b) and (c) with two different pitch sizes), respectively. (d) Luminescence light from a 150 mm wafer (exposed to UV light) with p-micropores(org/FA) etched through a nitride mask, demonstrating the homogeneity of the etching and, for the first time, micropores obtained with org electrolytes. Note that the structures in the quadrants are different.

1111 present the salient features of the CBM without justification of single issues. For details, the reader is  
 1112 referred to [9,10,12,20].

1113 When considering the electrochemistry of Si, it is always assumed (usually without even  
 1114 mentioning) that current flow is homogeneous in time and space. In other words, there is a well  
 1115 defined current density  $j(x, y, t)$  on the electrode at any point in space and time which will only change  
 1116 smoothly from point to point. This, however, is intrinsically impossible for the following reasons.

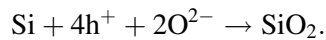
1117 Any electrochemical process that dissolves Si involves four distinctly different net chemical  
1118 reactions.

1119 1. *Direct dissolution* with the net reaction:



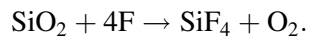
1122 where  $x$  holes ( $\text{h}^+$ ) are consumed in the reactions (and  $x$  must be  $\geq 1$ ), while  $y$  injected electrons  
1124 ( $\text{e}^-$ ) account for the rest of the charge needed. Direct dissolution thus makes the most efficient  
1125 use of holes; it can proceed if only one hole is supplied.

1126 2. *Oxidation* with the net reaction:



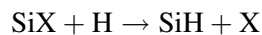
1129 Oxidation will always need four holes; it is thus not as efficient in the use of available holes as  
1131 direct dissolution.

1132 3. *Oxide dissolution* with the net reaction:



1135 Oxide dissolution is a purely chemical process that does not need current flow or applied  
1137 potentials. It essentially limits the total current that the system can process, because the oxide  
1138 generation rate cannot be larger than the dissolution rate (on average).

1139 4. *Hydrogen coverage* of the free Si surface, described by the formal (but useless) net reaction:



1142 It means that whatever is sitting on the surface will be replaced by hydrogen in due time as given  
1144 by some reaction constant  $k_{\text{cov}}$  as long as no other reactions take place. Far more important,  
1145 however, than the simple coverage of the surface with hydrogen, is the concurrent removal (or  
1146 *passivation*) of interface states having a certain density  $\rho(E)$  in the band-gap of the Si which  
1147 might also be described by first order reaction kinetics

$$1148 \quad \frac{d\rho(E)}{dt} = \rho_0 \exp(-k_{\text{pas}}t) \quad (7.1)$$

1150 and  $k_{\text{pas}}$  = reaction constant =  $k_{\text{pas}}$  (orientation, chemistry,  $T$ ). Note that  $k_{\text{pas}}$  is not identical to  
1152  $k_{\text{cov}}$ ! In the CBM, the reaction constant  $k_{\text{pas}}$  plays a major role in pore formation and while it is  
1153 generally not known, it is a measurable quantity.

1154 Looking at a typical macropore growth situation, it is clear that both dissolution processes must  
1155 occur simultaneously since the valence for the processes (i.e. the number of carriers flowing through  
1156 the external circuit for one atom of Si dissolved) is usually around 2.7 and a single process should  
1157 have an integer as valence. Oxide dissolution then is required, too, and, since the pore walls are  
1158 obviously not carrying current, the H-passivation process must also be present. Obviously, the four  
1159 processes cannot all occur at the *same time and at the same place*—totally homogeneous current  
1160 flow is intrinsically impossible.

1162 The problem could be swept under the rug by postulating that all processes occur at a very  
1163 small scale with defined, but totally uncorrelated probabilities. Averaging over small, but not too  
1164 small distances and times then would produce homogeneity in time and space, whereas  
1165 inhomogeneities on a large-scale—as expressed in current oscillations and pores—could still be



1166 possible. There is, however, no justification for this approach, even if that was the implicit  
1167 hypotheses all along.

1168 The current burst model goes to the other extreme and postulates that there are definite  
1169 correlations between the four basic processes. It has three major postulates as follows.

- 1170 1. Charge transfer and thus current flow is inherently inhomogeneous in time and space; in  
1171 particular there are times when no charge is transferred in some areas at some time. A charge  
1172 transfer process nucleates at  $(x, y, t)$  on the Si surface (or through a thin oxide) with a certain  
1173 probability,  $p$  that depends on the surface “state”  $S$  at  $(x, y, t)$ , but with an intrinsically stochastic  
1174 probability element. The sequence of events started in this way is called a *current burst*.
- 1175 2. The sequence of events in a current burst is dictated by logic. It must start with direct dissolution,  
1176 followed by oxidation, followed by oxide dissolution, and, if a new current burst does not nucleate  
1177 immediately, by hydrogen passivation. The lateral extension of a current burst is in the nm regime.
- 1178 3. Individual current bursts may interact in space and time. This means that the nucleation  
1179 probability,  $p$  of a current burst is not only a function of the surface state  $S(x, y, t)$  but may depend  
1180 on what has happened *before* at  $(x, y)$ —interaction in time—or on what is going on in the  
1181 *neighborhood* at  $t$ —interaction in space. Assuming that the interaction in space and in time can be  
1182 separated, we have

1183

$$p(x, y, t) = \int_{x \pm \Delta x, y \pm \Delta y} \int \mathrm{d}\tilde{x} \mathrm{d}\tilde{y} \int_0^t \mathrm{d}\tilde{t} W_r(x - \tilde{x}, y - \tilde{y}) \times W_t(t - \tilde{t}) \times S(\tilde{x}, \tilde{y}, \tilde{t}). \quad (7.1)$$

1185

1186 The essential parts are the functions  $W$  which contain the possible interactions in space and time  
1187 and which will only be considered qualitatively in what follows. There are several ways in which  
1188 current bursts can interact in space or time. First, we consider interaction in space.

1189 One mechanism is described in detail in [23,24] and may be envisioned as follows: a current  
1190 burst that nucleates between the oxide patches produced by two older ones has to produce less oxide  
1191 before the field strength is low enough to stop oxidation. It interacts in space, but its behavior (the  
1192 “switching off” and similarly, the “switching on”) is correlated in time to its neighbors. *Interaction*  
1193 in space thus results in a *correlation* in time, and if this interaction spreads by some percolation  
1194 mechanism, areas of the electrode characterized in size by some correlation lengths  $L_{CO}$ , fire and  
1195 quench their current bursts in (stochastic, i.e. never perfect) synchronization. This means that  
1196 *domains* with a size given by  $L_{CO}$  are formed that erode the Si surface in a synchronized way.

1197 Obviously, this interaction mechanism needs some minimum of oxidation, current densities not  
1198 too low (so that current bursts have to nucleate in a density high enough to enable next neighbor  
1199 interaction and some percolation), and oxide dissolution rates not too large. If the correlation length  
1200  $L_{CO}$  (a major quantity of the CBM) becomes comparable to the specimen size, macroscopic current  
1201 oscillations will result [19]. Further interaction mechanisms are conceivable, but it does not matter  
1202 for the essentials of the CBM exactly how interaction in space takes place.

1203 Interaction in time is easy to visualize: if the nucleation probability  $p$  for a current burst depends  
1204 on the potential or field strength at the interface, it will decrease with an increasing amount of  
1205 passivation because passivation, as pointed out in Section 2.3, lowers the surface potential by  
1206 allowing a space charge region to develop. Surfaces where no current bursts happened for some time  
1207 are more passivated and thus less likely to nucleate a new CB. Turned around, CBs are more likely to  
1208 nucleate where another CB took place not too long ago—there is an interaction in time. If strong  
1209 enough, it will tend to cluster CBs in areas where other CBs were prominent—either because current  
1210 was originally confined to some special places by using lithographically defined nucleation, or

1211 because random fluctuations eventually cause precipitation of CBs. Since the kinetics of passivation  
1212 are strongly anisotropic (cf. Section 2.3), so is CB nucleation, and CBs nucleate preferentially on  
1213  $\{1\ 0\ 0\}$  (and  $\{1\ 1\ 3\}$ ) surfaces. *Interaction* in time thus leads to a *correlation* in space and CBs  
1214 correlated in space are CB clusters which produce pores.

1215 Pores with anisotropic behavior, under quite general circumstances, are thus a natural  
1216 consequence of the CBM. Put in different words, stochastic interactions between localized events  
1217 will under very general circumstances lead to a *phase separation* in the system: parts of the electrode  
1218 contain many CBs and draw the highest current density possible under the circumstances, whereas  
1219 other parts of the electrode are completely inert.

1220 There are more types of correlations possible and the morphology (and to a lesser extent the  
1221 geometry) of the pores can be linked to the dominating correlation.

- 1223 • An “anti correlation” (meaning that the nucleation probability is highest wherever CBs have not  
1224 happened before), together with quantum dot effects, produces micropores. This means that CB  
1225 nucleate as soon as possible, i.e. right after oxide removal (most likely between some former  
1226 bursts where the oxide was thinnest). This will draw a maximum of current because the active  
1227 surface in this case will fold and thus is larger than the nominal surface. A sponge-like structure,  
1228 not dependent on the crystal orientation, results with a porosity that increases with the current  
density—in other words we observe micropores.
- 1230 • A positive interaction in time but without the formation of synchronized domains (or only very  
1231 small domains), i.e. with no strong interaction in space, will produce mesopores. Current bursts  
1232 eventually cluster and form pores with larger diameters. Avoidance of domains means insufficient  
1233 oxidation and that can be seen as the common denominator of mesopores: they always form if the  
1234 oxidation reaction is weak and direct dissolution is dominant. This may be induced by a lack of  
1235 holes or weakly oxidizing electrolytes. Lack of holes is not an absolute measure but is defined  
1236 relative to the amount of holes that electrolyte can process by direct dissolution. Increasing the  
1237 doping of p-Si, e.g. increases the hole supply but because the potential at the interfaces increases  
1238 too (less voltage drop in the SCR), the ability to use up holes in direct dissolution increases faster  
1239 than the hole supply—in p<sup>+</sup> Si (and, in the same vein, n and n<sup>+</sup> Si in the dark) the oxidation  
reaction tends to be suppressed.
- 1241 • Macropores form if sizeable domains are possible, i.e. if a minimum of oxidation permits  
1242 interactions in space in addition to interaction in time. The morphology of the pores then is mainly  
1243 determined by the mixture of length scales present. Only if the domain size and the other length  
1244 scales (e.g. the SCR width in the case of n-macropores(aqu/bsi)) are close to each other, “perfect”  
1245 macropores will result.

1246 Before these somewhat abstract concepts will be applied to the more puzzling cases shown in  
1247 the preceding chapters, some unique features of the CBM must be discussed. It does not only  
1248 introduce an *intrinsic length scale* (the domain size  $L_{CO}$ ), but also several *intrinsic time scales*. In  
1249 particular, we have listed as follows.

- 1251 • The average duration  $\tau_{CB}$  of a CB. It is the sum of the average times for direct dissolution, oxidation,  
1252 oxide dissolution and hydrogen passivation and determines directly the frequency of current or  
1253 voltage oscillations. In many cases, the time for oxide dissolution will be the largest time in this  
sequence and a lower limit for  $\tau_{CB}$  can than be obtained from the oxide dissolution kinetics.
- 1255 • The average time  $\tau_{DS}$  for the loss of synchronization between domains that started in phase. This  
1256 is the mechanism that leads to damped current oscillations observed if the system is abruptly  
turned to some high voltage. The value of  $\tau_{DS}$  can be considerably longer than  $\tau_{CB}$ .

- The time  $\tau_L$  it takes for a given pore to grow one correlation length  $L_{CO}$  into the depth of the sample. It has an important consequence: at least the time  $\tau_L$  has to elapse before a (new) side pore can be dug into a pore wall by a domain of the size  $L_{CO}$ .

The CBM thus supplies intrinsic time scales and therefore the necessary ingredient for any kind of non-linear or resonant behavior if external time scales (e.g. the frequency of current modulations) are forced on the system.

### 7.2. The hammer model

For the case of macropores, the CBM can be expressed in a simple analogy, the “hammer model”: macropores are formed by “hammering” them out of the silicon with a hammer that has the average size of a domain, i.e.  $L_{CO}$ . This hammer bangs away with the frequency  $1/\tau_{CB}$  and every blow removes a patch of Si with a thickness corresponding to the average depth of a current burst. This is illustrated in Fig. 27.

The probability of a hammer strike is give by the nucleation probability of a current burst—the hammer will tend to strike on “soft” parts of the pore more often than on hard parts. At this stage, the correlations between current bursts are already part of the model (a pore has formed and a domain with defined size exists), the nucleation probability is now that of a whole domain. It depends, of course, on the carrier supply (CBs that nucleate but find no carriers will not “take”) and on the passivation stage. Space charge regions, not containing carriers, thus are very hard, as are  $\langle 111 \rangle$  directions, while  $\langle 100 \rangle$  directions are “soft” and  $\langle 113 \rangle$  directions are not too hard, either.

We now can distinguish three basic cases: the hammer is smaller, larger, or comparable to the pore size (which might be determined by some of the other length scales of the system). This is shown in Fig. 28.

Case (a)—domain size larger than pore size—is obviously not possible! This explains why macropores with small diameters are so difficult to make—it is not only the width of the SCR that counts, but also the domain size.

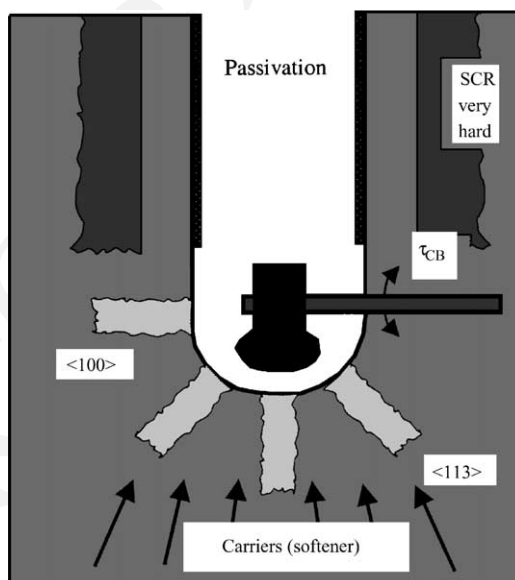


Fig. 27. The “hammer model”. Silicon is always removed in patches corresponding to the domain size of the system.

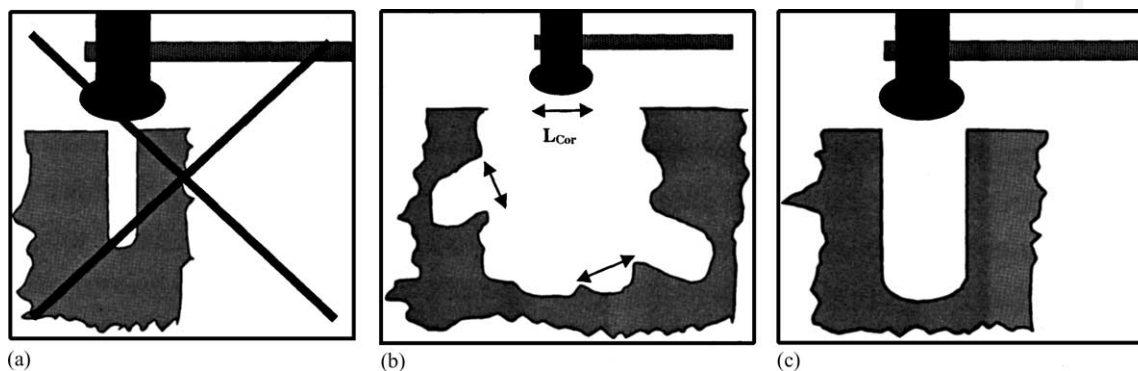


Fig. 28. Domain size and pore morphology. Case (a) is not possible; case (b) yields bulgy or branched pores and case (c) perfect pores.

Case (b)—making a large pore with one (or several) small hammers will produce rough pore wall or even branching. Note that the size of branches reflect the hammer size, and that a hammer, after striking off a side pore, will be trapped in this pore. It is also clear that a new side pore can only be formed if the main pore grew at least one hammer size into the depth and if that part of the pore wall is not sufficiently passivated yet.

Case (c)—simply gives “perfect pores”. The hammer can only strike the bottom, each blow removes the same patch—the diameter is constant and no side pores are formed.

The simple hammer model explains easily most of the observations concerning all kinds of macropores. In particular, it is clear why very thin n-macropores(aqu/bsi) cannot be made and why the pores become very rough with increasing diameter (cf. Fig. 4). Very perfect pores mean that everything has to be just right. Changing parameters a little bit, e.g. the HF concentration from 4% where perfect n-macropores(aqu/bsi) result to, say 7% in order to increase the etch rate somewhat, will result in less perfect pores with rougher pore walls—as always observed.

The hammer model predicts exactly what is seen for the p-macropores(aqu) case shown in Fig. 10a and b. The natural size of the p-macropore(aqu) is given by the hammer size, the wall thickness corresponds to the SCR width. If the pores are forced to grow with larger diameters, the “hammers” become visible as bulges at the pore tip with dimensions identical to that of the size if randomly nucleated pores. Random nucleation, in this context, means that a domain stays in one area long enough (is “pinned”) so that the proto-pore it produces effectively leads to self-pinning: the domain falls into the pit it dug itself!

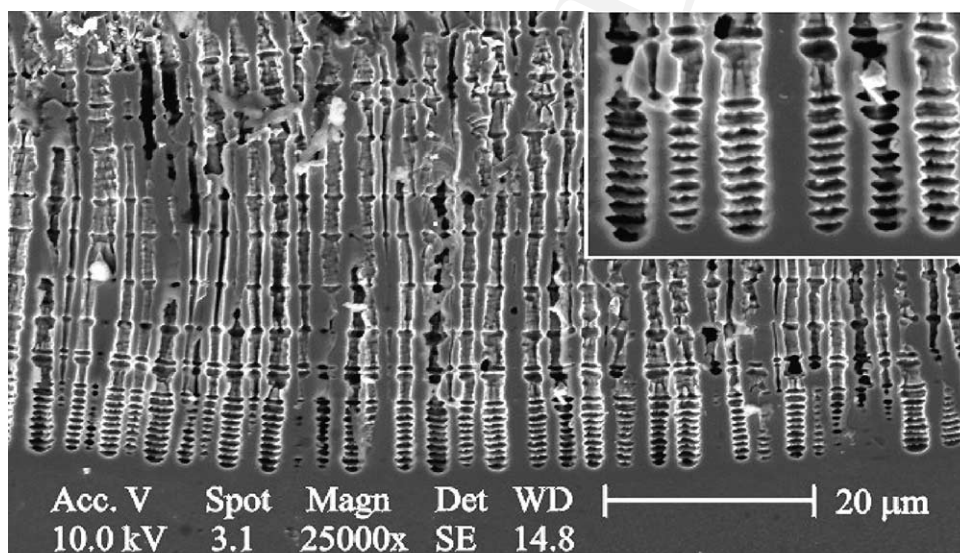
The dependence of p-macropores(org) on the oxidizing power of the electrolyte and so on can be understood in principle, and, particularly interesting, the strange behavior of n-macropores(org/bsi) may be interpreted. Since the oxidation power of organic electrolytes is generally smaller than that of aqu electrolytes, it is reduced even more if the hole supply now is limited too, for n-type Si. The correlation length decreases—the hammer becomes smaller. We now have the case shown in Fig. 28b since the average pore distance is still dictated by SCR properties and the current flowing through the system thus must produce pores with diameters large than the hammer size.

Generally, side pores tend to form if a) one or a few small hammers must produce a big pore, and b) the H-passivation of the side walls is so slow that a hammer can still attack the side walls above the pore tip (then most likely the {1 0 0} or {1 1 3} surfaces oriented into the direction of hole supply). The second condition demands that the pore has-grown about one correlation length into the depth since the last branching in order to supply sufficient wall area. If these conditions are met,

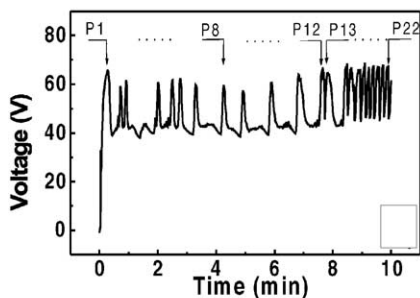


1316 three predictions emerge: (1) the diameter of the side pores is comparable to that of the main pore  
 1317 and given by the hammer size, i.e. the correlation length  $L_{CO}$ ; (2) branches will be relatively regular  
 1318 and at a distance corresponding to the correlation length; (3) branching can be suppressed if the  
 1319 current density is periodically reduced with a frequency somewhat larger than  $1/\tau_L$  with  $\tau_L$ , as  
 1320 defined above = time to grow the pore a distance  $L_{CO}$  into the depth of the sample. This is to be  
 1321 expected because decreasing the current (which, at least under back side illumination conditions,  
 1322 always is focussed on the pore tip) forces the domains back to the pore tip and thus gives the side  
 1323 walls more time to passivate.

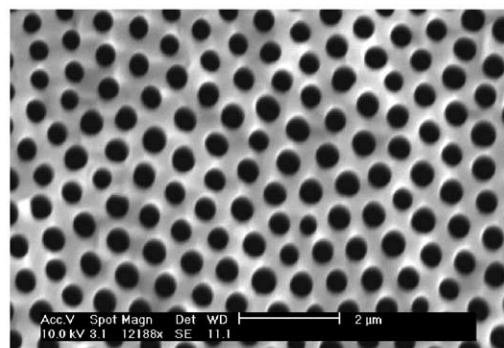
1324 In summary, while the “hammer model” is certainly oversimplified, the general stochastic  
 1325 approach to electrochemistry of Si is not. While it still has loose ends and needs to be worked out in  
 1326 detail, it already supplies explanations of observed phenomena not obtainable in other models,  
 1327 predicts to a certain extent the outcome of experiments not yet performed, and, most valuable, gives  
 1328 concrete guidance for the design of electrolytes and experiments with a specific goal in mind.



(a)



(b)



(c)

Fig. 29. Macropores in InP obtained in an HCl electrolyte (n-type, doping level =  $1.5 \times 10^{16} \text{ cm}^{-3}$ ,  $j = 100 \text{ mA/cm}^2$ ). (a) Macropores with periodic diameter oscillations, (b) voltage oscillations with peaks corresponding to the diameter oscillations, (c) top view showing tendency to form a hexagonal pore lattice (from [96]).

### 7.3. Pores in III–V compounds

It is possible to obtain electrochemically etched pores in III–V compounds, too, cf. [26–31]. In particular, pores in GaAs, GaP, and InP have been investigated, but much of the parameter space has not yet been systematically explored. While pores in these materials are often very different in their general appearance from pores in Si, there are some similarities, too.

A particular interesting feature is that while current or voltage oscillations akin to those in Si in the electropolishing regime have not been observed, voltage oscillations have recently been found to occur during macropore etching in all three materials mentioned [106], Fig. 29 shows some examples.

Similar results have been obtained in GaP and GaAs samples. The CBM maintains that the stochastic processes governing current and voltage oscillations in Si are essentially also responsible for pore formation in other semiconductors. Macroscopic oscillations and pore formation, however, have never been observed together in Si. Their occurrence in III–V compounds, nevertheless, adds credibility to basic assumptions of the CBM; a detailed analysis, however, will transgress the intentions of this paper and will be published elsewhere.

### Acknowledgements

The authors are indebted V. Lehmann, S. Rönnebeck, F. Müller, S. Langa and I.M. Tiginyanu who supplied some of their pictures for inclusion in this review and were valued partners in many stimulating meetings. Invigorating discussions with R. Wehrspohn, J.-N. Chazalviel and F. Ozanam concerning the electrochemistry of silicon and pore formation are gratefully acknowledged. G. Popkirov and J. Bahr supplied the experimental help and the special equipment for many experiments.

### References

- [1] L.T. Canham, *J. Appl. Phys. Lett.* 57 (1990) 1046.
- [2] V. Lehmann, U. Gösele, *J. Appl. Phys. Lett.* 58 (1991) 856.
- [3] V. Parkhutik, *Solid State Electron.* 43 (1999) 1121–1141.
- [4] M.P. Stewart, J.M. Buriak, *Adv. Mater.* 12 (2000) 859.
- [5] M.J. Sailor, Sensor application of porous silicon, in: L.T. Canham (Ed.), *Properties of Porous Silicon*, IEE-Books, London, 1997.
- [6] L.T. Canham, Biomedical applications of porous silicon, in: L.T. Canham (Ed.), *Properties of Porous Silicon*, IEE-Books, London, 1997.
- [7] T. Yonehara, BESOI with porous silicon: ELTRAN, in: L.T. Canham (Ed.), *Properties of Porous Silicon*, IEE-Books, London, 1997.
- [8] M.G. Berger, M. Thönissen, W. Theiß, H. Münder, Microoptical devices based on porous silicon, in: M.O. Manasreh (Ed.), *Optoelectronic Properties of Semiconductors and Superlattices*, vol. 5, Gordon and Breach, Amsterdam, 1997.
- [9] J. Carstensen, M. Christophersen, H. Föll, *Mater. Sci. Eng. B* 69/70 (2000) 23.
- [10] J. Carstensen, M. Christophersen, G. Hasse, H. Föll, *Phys. Solid State (a)* 182 (2000) 63.
- [11] G. Hasse, J. Carstensen, G.S. Popkirov, H. Föll, *Mater. Sci. Eng. B* 69/70 (2000) 188.
- [12] H. Föll, J. Carstensen, M. Christophersen, G. Hasse, *Phys. Solid State (a)* 182 (2000) 7.
- [13] H. Föll, V. Lehmann, European Patent EP0400387B1 (1990).
- [14] E. Yablonovitch, D.L. Allara, C.C. Chang, T. Gmitter, T.B. Bright, *Phys. Rev. Lett.* 57 (1986) 249.
- [15] V. Lehmann, H. Föll, *J. Electrochem. Soc.* 135 (1988) 2831.
- [16] J. Carstensen, W. Lippik, H. Föll, *ECS Proceedings*, vol. 94-10, San Francisco, 1994, p. 1105.
- [17] H. Föll, *J. Appl. Phys.* 53A (1991) 8.

- 1374 [18] G. Mende, E. Hensel, *Thin Solid Films* 168 (1989) 51.
- 1375 [19] G. Hasse, J. Carstensen, H. Föll, in: P. Schmuki, D.J. Lockwood, Y.H. Ogata, H.S. Isaacs (Eds.), *ECS Proceedings*,  
1376 2001, submitted for publication.
- 1377 [20] H. Föll, J. Carstensen, M. Christophersen, G. Hasse, in: P. Schmuki, D.J. Lockwood, Y.H. Ogata, H.S. Isaacs (Eds.),  
1378 *Pits and Pores II: Formation Properties and Significant for Advanced Materials*, Electrochemical Society Meeting  
1379 *Proceedings*, 2001, p. 36.
- 1380 [21] S. Rönnebeck, J. Carstensen, S. Ottow, H. Föll, *Electrochem. Solid State Lett.* 2 (1999) 126.
- 1381 [22] M. Christophersen, J. Carstensen, A. Feuerhake, H. Föll, *Mater. Sci. Eng. B* 69/70 (2000) 194.
- 1382 [23] J. Carstensen, R. Prange, H. Föll, *J. Electrochem. Soc.* 146 (1999) 1134.
- 1383 [24] J. Carstensen, R. Prange, G.S. Popkirov, H. Föll, *J. Appl. Phys. A* 67 (1998) 459.
- 1384 [25] O. Jessensky, F. Müller, U. Gösele, *J. Electrochem. Soc.* 145 (1998) 3735.
- 1385 [26] P. Schmuki, J. Fraser, C.M. Vitus, M.J. Graham, *J. Electrochem. Soc.* 143 (1996) 3316–3322.
- 1386 [27] S. Langa, J. Carstensen, M. Christophersen, H. Föll, I.M. Tiginyanu, *J. Appl. Phys. Lett.* 78 (2001) 1074–1076.
- 1387 [28] B.H. Erne, D. Vanmaekelbergh, J.J. Kelly, *J. Electrochem. Soc.* 143 (1996) 305–314.
- 1388 [29] M.A. Stevens-Kalceff, S. Langa, I.M. Tiginyanu, J. Carstensen, M. Christophersen, H. Föll, in: P.M. Fauchet, J.M.  
1389 Buriak, L.T. Canham, N. Koshida, B.E. White Jr. (Eds.), *Microcrystalline and Nanocrystalline Semiconductors*.  
1390 *Mater. Res. Soc. Symp. Proc.* (638) 2001.
- 1391 [30] T. Takizawa, S. Arai, *Jpn. J. Appl. Phys.* 54 (1994) L643.
- 1392 [31] S. Langa, I.M. Tiginyanu, J. Carstensen, M. Christophersen, H. Föll, *J. Electrochem. Solid State Lett.* 3 (2000) 514.
- 1393 [32] V.P. Parkhutik, E. Matveeva, *Electrochem. Solid State Lett.* 2 (1999) 371.
- 1394 [33] E.K. Propst, P.A. Kohl, *J. Electrochem. Soc.* 141 (1994) 1006.
- 1395 [34] M. Christophersen, J. Carstensen, H. Föll, *Phys. Solid State (a)* 182 (2000) 45.
- 1396 [35] V. Lehmann, H. Föll, *J. Electrochem. Soc.* 137 (1990) 653.
- 1397 [36] V. Lehmann, *J. Electrochem. Soc.* 140 (1993) 2836.
- 1398 [37] V. Lehmann, W. Hönlein, H. Reisinger, A. Spitzer, H. Wendt, J. Willer, *Solid State Technol.* 38 (1995) 99.
- 1399 [38] V. Lehmann, U. Grüning, *Thin Solid Films* 297 (1997) 13–17.
- 1400 [39] M. Hejjo Al Rifai, M. Christophersen, S. Ottow, J. Carstensen, H. Föll, *J. Electrochem. Soc.* 147 (2000) 627.
- 1401 [40] M.J.J. Theunissen, *J. Electrochem. Soc.* 119 (1972) 351.
- 1402 [41] V. Lehmann, S. Stengl, A. Luigart, *Mater. Sci. Eng. B* 69/70 (2000) 11.
- 1403 [42] J.-N. Chazalviel, R. Wehrspohn, F. Ozanam, *Mater. Sci. Eng. B* 69/70 (2000) 1.
- 1404 [43] R.L. Smith, S.D. Collins, *J. Appl. Phys.* 71 (1992) R1.
- 1405 [44] V. Lehmann, U. Gösele, *Adv. Mater.* 4 (1992) 114.
- 1406 [45] F. Müller, A. Birner, J. Schilling, R.B. Wehrspohn, U. Gösele, *Adv. Solid State Phys.* 40 (2000) 545.
- 1407 [46] U. Grüning, *Ph.D. Thesis*, Erlangen, 1997.
- 1408 [47] P. Kleinmann, J. Linnros, S. Petersson, *Mater. Sci. Eng. B* 69/70 (2000) 29.
- 1409 [48] F. Müller, A. Birner, J. Schilling, U. Gösele, C. Kettler, P. Hänggi, *Phys. Solid State (a)* 182 (2000) 585.
- 1410 [49] J.E.A.M. van den Meerakker, R.J.G. Elfrink, F. Roozeboom, J.F.C.M. Verhoeven, *J. Electrochem. Soc.* 147 (2000)  
1411 2757.
- 1412 [50] M. Christophersen, P. Merz, J. Quenzer, J. Carstensen, H. Föll, *Sens. Actuators A* 88 (2001) 241.
- 1413 [51] M. Christophersen, J. Carstensen, H. Föll, *Phys. Solid State (a)* 182 (2000) 601.
- 1414 [52] M.M. Rieger, P.A. Kohl, *J. Electrochem. Soc.* 142 (1995) 1490.
- 1415 [53] E.A. Ponomarev, C. Levy-Clement, *J. Electrochem. Soc. Lett.* 1 (1998) 1002.
- 1416 [54] M. Christophersen, J. Carstensen, H. Föll, *Phys. Solid State (a)* 182 (2000) 103.
- 1417 [55] H. Ohji, P.J. French, K. Tsutsumi, *Sens. Actuators A* 82 (2000) 254.
- 1418 [56] K.J. Chao, S.C. Kao, C.M. Yang, M.S. Hseu, T.G. Tsai, *Electrochem. Solid State Lett.* 3 (2000) 489.
- 1419 [57] C. Levy-Clement, A. Lagoubi, M. Tomkiewicz, *J. Electrochem. Soc.* 141 (1971) 958.
- 1420 [58] R.L. Meek, *Surf. Sci.* 25 (1971) 526.
- 1421 [59] A. Valance, *Phys. Rev. B* 52 (1995) 8323.
- 1422 [60] V. Lehmann, S. Rönnebeck, *J. Electrochem. Soc.* 146 (1999) 2968.
- 1423 [61] V. Lehmann, R. Stengl, A. Luigart, *Mater. Sci. Eng. B* 69/70 (2000) 11.
- 1424 [62] S. Ottow, V. Lehmann, H. Föll, *J. Electrochem. Soc.* 143 (1996) 385.
- 1425 [63] S. Ottow, V. Lehmann, H. Föll, *Appl. Phys. A* 63 (1996) 153.
- 1426 [64] J. Rousselet, L. Salomone, A. Ajdari, J. Proust, *Nature* 370 (1994) 446.
- 1427 [65] C. Kettner, P. Reimann, P. Hänggi, F. Müller, *Phys. Rev. E* 61 (2000) 212.
- 1428 [66] V. Lehmann, S. Rönnebeck, *Sens. Actuators A* 95 (2001) 202.
- 1429 [67] M. Bengtsson, S. Ekstöm, J. Drott, A. Collins, E. Csöregi, G. Marko-Varga, T. Laurell, *Phys. Stat. Sol.* 182 (2000)  
1430 495.
- 1431 [68] V. Lehmann, S. Ottow, R. Stengl, H. Reisinger, H. Wendt, *European Patent WO9961147* (1999).
- 1432 [69] V. Lehmann, *Electrochemistry of Silicon*, Wiley-VCH, Weinheim, 2002.
- 1433 [70] R. Angelucci, A. Poggi, L. Dori, A. Tagliani, G.C. Cardinali, F. Corticelli, M. Madisaldi, *J. Porous Mater.* 7 (2000)  
1434 197.

- 1435 [71] E.V. Astrova, V.B. Voronkov, I.V. Grekov, *Tech. Phys. Lett.* 25 (1999) 958.  
1436 [72] H. Föll, V. Lehmann, European Patent EP0296348B1 (1993).  
1437 [73] V.V. Starkov, E.Y. Gavrilin, J. Konle, H. Presting, A.F. Vyatkin, U. König, *Phys. Solid State (a)*, 2000, in press.  
1438 [74] H. Föll, J. Grabmaier, V. Lehmann German Patent DE 3324232 C2 (1983).  
1439 [75] A. Prasad, S. Balakrishnan, S.K. Jain, G.C. John, *J. Electrochem. Soc.* 129 (1982) 596.  
1440 [76] M. Liponski, P. Panek, S. Bastide, C. Levy-Clement, *Phys. Solid State (a)*, 2002, in press.  
1441 [77] E.A. Ponomarev, C. Levy-Clement, *J. Porous Mater.* 7 (2000) 51.  
1442 [78] S.R. Nicewarner-Pena, R.G. Freeman, B.D. Reiss, L. He, D.J. Pena, I.D. Walton, R. Cromer, C.D. Keating, M.J. Natan, *Science* 294 (2001) 137.  
1443 [79] E. Yablonovitch, *Phys. Rev. Lett.* 58 (1987) 2059.  
1444 [80] S. John, *Phys. Rev. Lett.* 58 (1987) 2486.  
1445 [81] U. Grüning, S. Ottow, V. Lehmann, *Appl. Phys. Lett.* 68 (1996) 747.  
1446 [82] A. Birner, K. Busch, F. Müller, *Phys. Biol.* 55 (1999) 27.  
1447 [83] F. Müller, A. Birner, U. Gösele, V. Lehmann, S. Ottow, H. Föll, *J. Porous Mater.* 7 (2000) 201.  
1448 [84] V. Lehmann, R. Stengl, H. Reisinger, R. Detempele, W. Theiss, *Appl. Phys. Lett.* 78 (2001) 589.  
1449 [85] P. Merz, European Patent DE 199,56,654 A1 (1999).  
1450 [86] C. Jäger, B. Finkenberger, W. Jäger, M. Christophersen, J. Carstensen, H. Föll, *Mater. Sci. Eng. B* 69/70 (2000) 199.  
1451 [87] R.B. Bergmann, T.J. Rinke, J.H. Werner, *Phys. Biol.* 56 (2000) 51.  
1452 [88] R. Brendel, R. Auer, *Phys. Phys. Solid State (a)*, 2002, in press.  
1453 [89] K. Sakaguchi, H. Kurisu, K. Ohmi, T. Yonahara, in: P. Schmuki, D.J. Lockwood, Y.H. Ogata, H.S. Isaacs (Eds.), *ECS Proceedings*, 2001, in press.  
1454 [90] K. Imai, H. Unno, *IEEE Trans. Electron Devices* 31 (1984) 297.  
1455 [91] W. Lang, in: M.O. Manasreh (Ed.), *Optoelectrical Properties of Semiconductors and Superlattices*, vol. 5, Gordon and Breach, Amsterdam, 1997.  
1456 [92] N. Koshida, H. Koyam, *Appl. Phys. Lett.* 60 (1992) 347.  
1457 [93] J. Buriak, M. Allen, *J. Lumin.* 80 (1999) 29.  
1458 [94] M. Thönissen, S. Billat, U. Frotscher, U. Rossow, M. Krüger, H. Tüth, M.G. Berger, *J. Appl. Phys.* 80 (1996) 2990.  
1459 [95] G. Lérondel, T. Yao, in: *proceedings of the PSST Conference (extended abstracts)*, 2000, p. 138.  
1460 [96] J.M. Buriak, *Adv. Mater.* 11 (1999) 265.  
1461 [97] S. Letant, M.J. Sailor, *Adv. Mater.* 12 (2000) 355.  
1462 [98] W. Lang, *Mater. Sci. Eng. R17* (1996) 1–55.  
1463 [99] L.T. Canham, *Adv. Mater.* 7 (1995) 1033.  
1464 [100] A.H. Mayne, S.C. Bayliss, P. Barr, M. Tobin, L.D. Backberry, *Phys. Stat. Sol.* 182 (2000) 505.  
1465 [101] L.T. Canham, R. Aston, J.-N. Chazalviel, C. Reeves, *Phys. Solid State (a)*, 2002, in press.  
1466 [102] C.C. Striemer, F. Fauchet, *Phys. Solid State (a)*, 2002, in press.  
1467 [103] D. Kovalev, V.Yu. Timoshenko, N. Künzner, E. Gross, F. Koch, *Phys. Rev. Lett.* 87 (2001) 068301.  
1468 [104] B.E. Collins, K.-P.S. Dancil, G. Abbi, M.J. Sailor, *Adv. Funct. Mater.* 12 (2002) 187.  
1469 [105] J.-N. Chazalviel, in: J.-C. Vial, J. Derrien (Eds.), *Porous Silicon Science and Technology*, Springer, Berlin, 1995, p. 17.  
1470 [106] S. Langa, J. Carstensen, I.M. Tiginyanu, M. Christophersen, H. Föll, *Electrochem. Solid State Lett.* 4 (2001) G50.